

Cross-correlation between CMB polarization and μ -distortion anisotropies

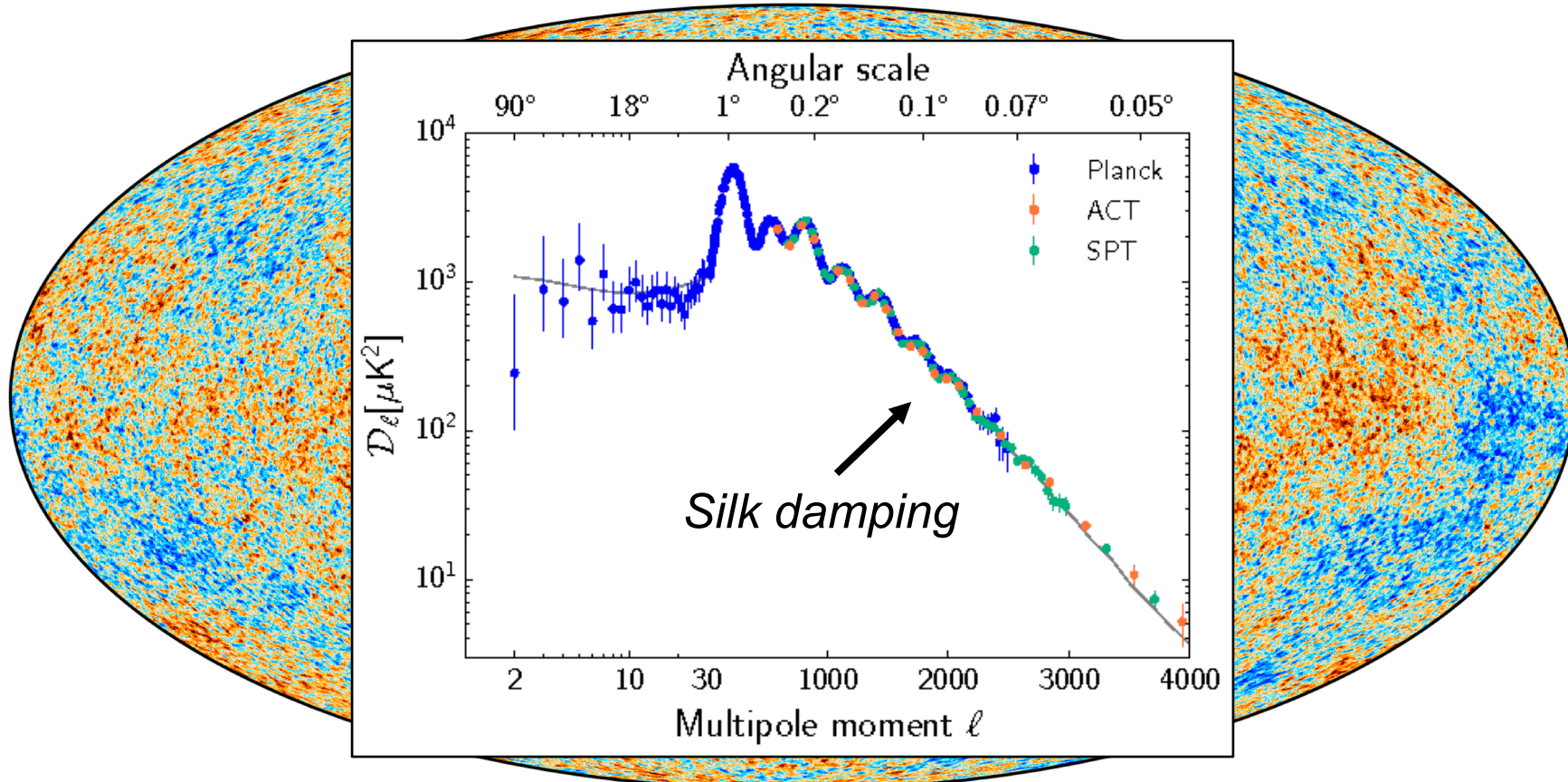
Mathieu Remazeilles
Jodrell Bank Centre for Astrophysics



The University of Manchester

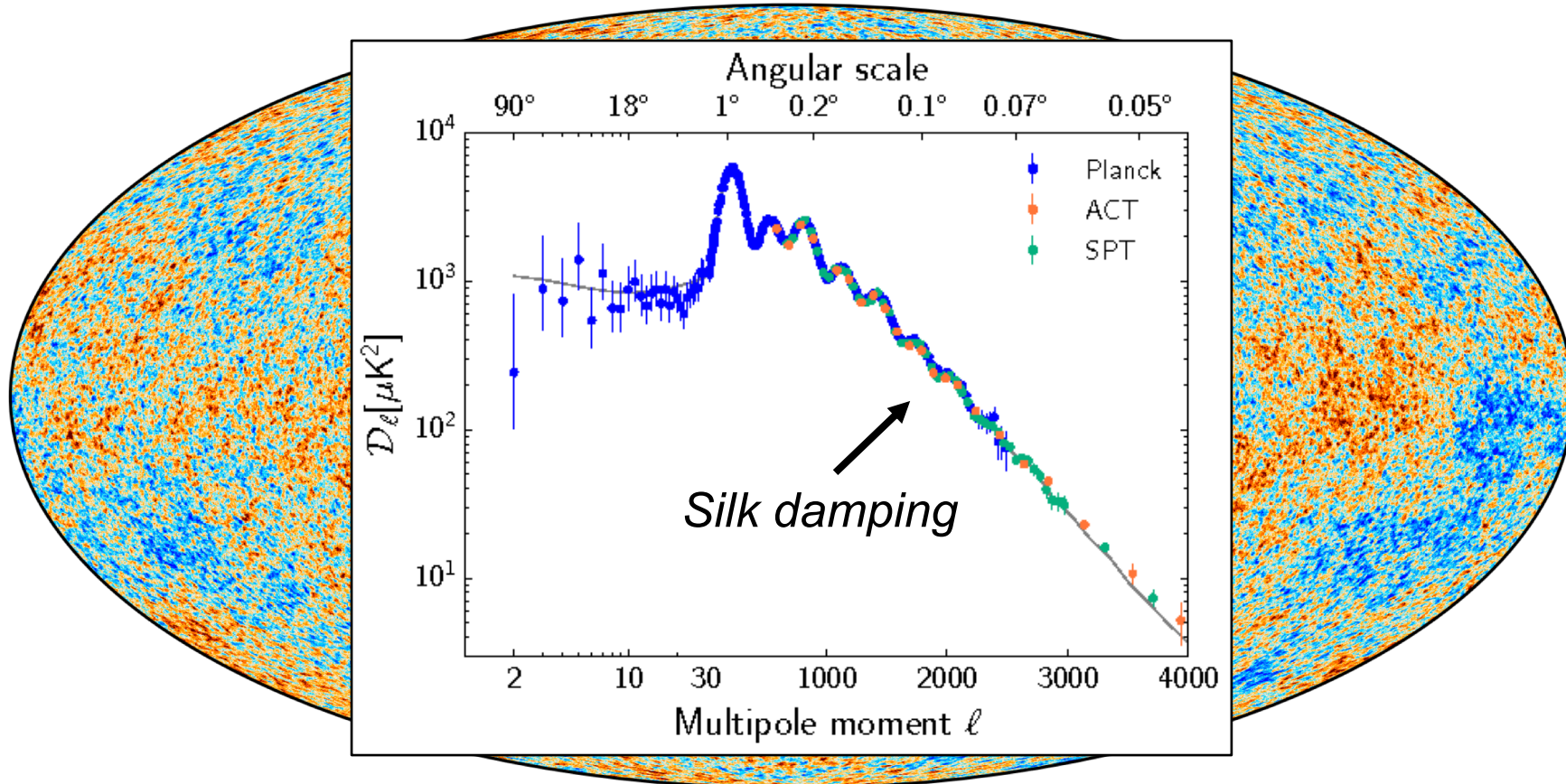
Remazeilles, Ravenni, Chluba, 2110.14664
Remazeilles & Chluba, MNRAS 2018

Dissipation of small-scale acoustic modes



Photons random-walk out of *overdense / hot* regions towards *underdense / cold* regions, thus uniformizing the temperature of small-scale regions foremost

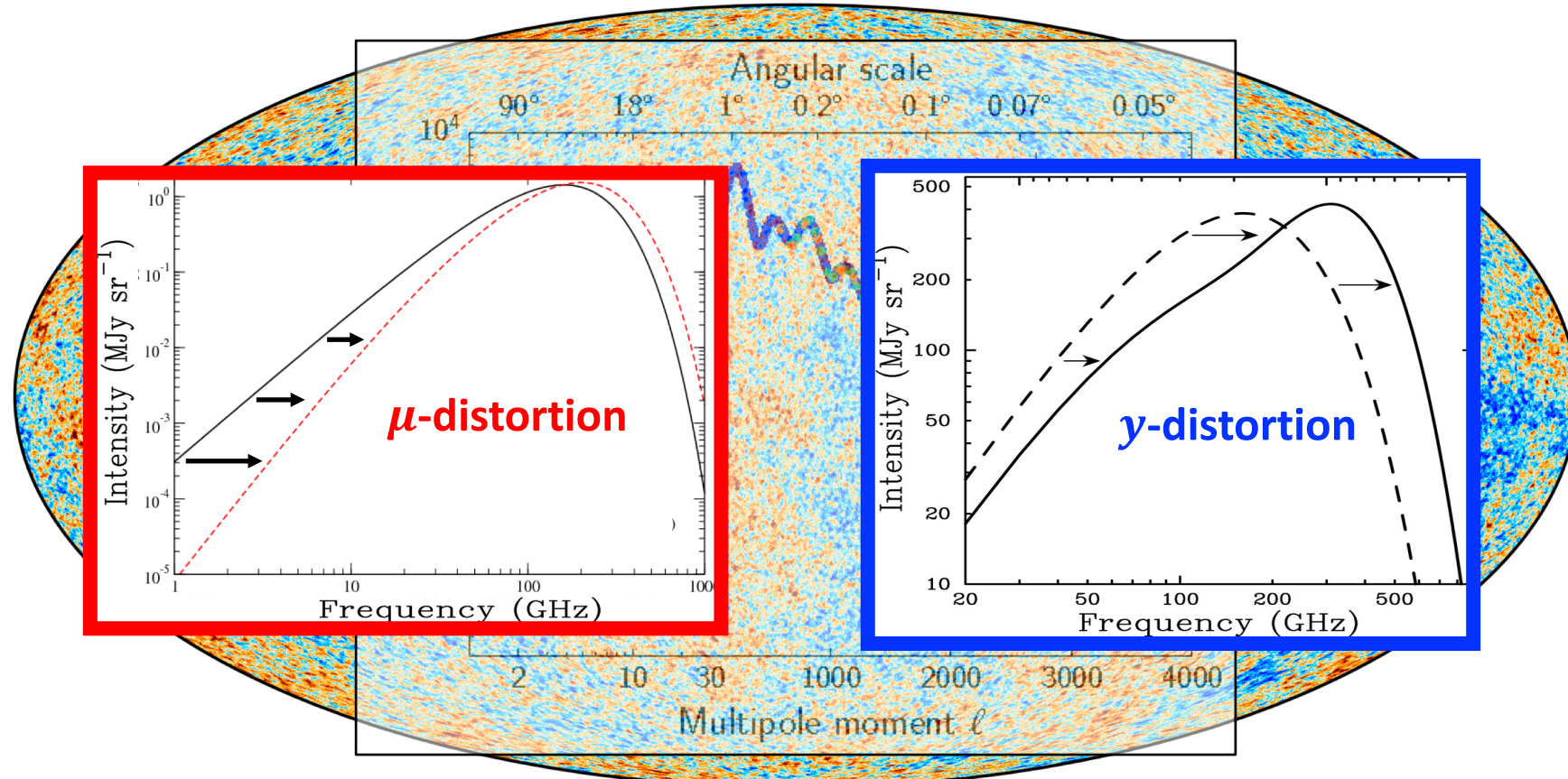
Dissipation of small-scale acoustic modes



Photons random-walk out of *overdense / hot* regions towards *underdense / cold* regions,
thus uniformizing the temperature of small-scale regions foremost

⇒ ***mixing blackbodies of different temperatures***

Dissipation of small-scale acoustic modes



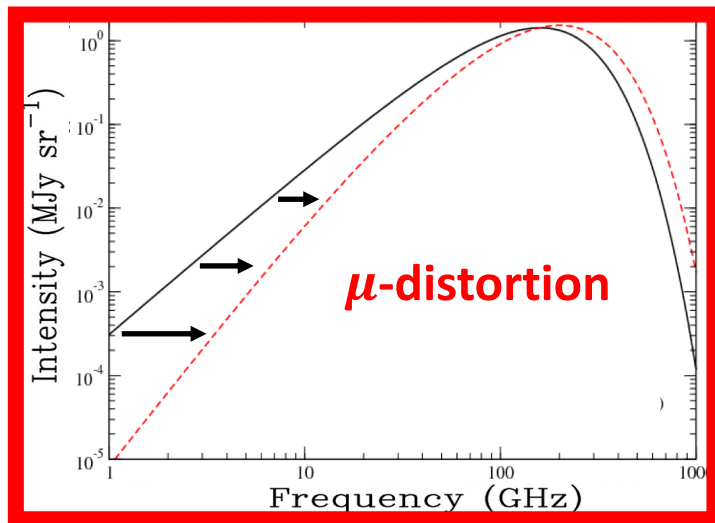
Photons random-walk out of *overdense / hot* regions towards *underdense / cold* regions,
thus uniformizing the temperature of small-scale regions foremost

⇒ ***mixing blackbodies of different temperatures***

CMB spectral distortions

Important at early times

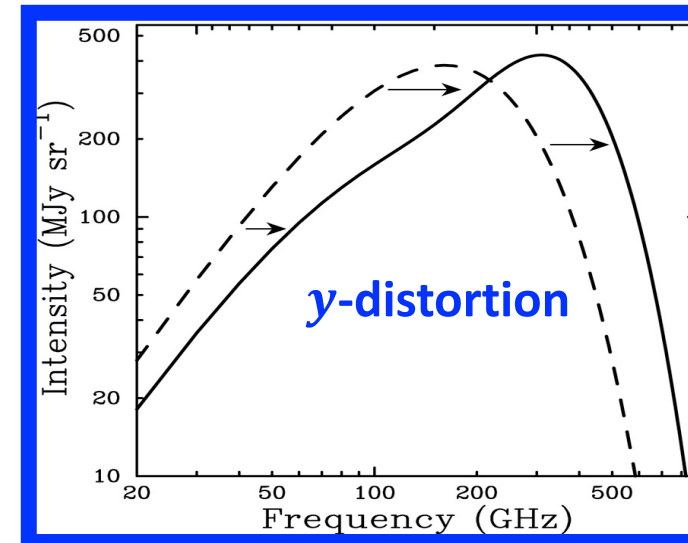
$$z > 10^4$$



Sunyaev & Zeldovich, ApSS (1970)

Important at late times

$$z < 10^4$$

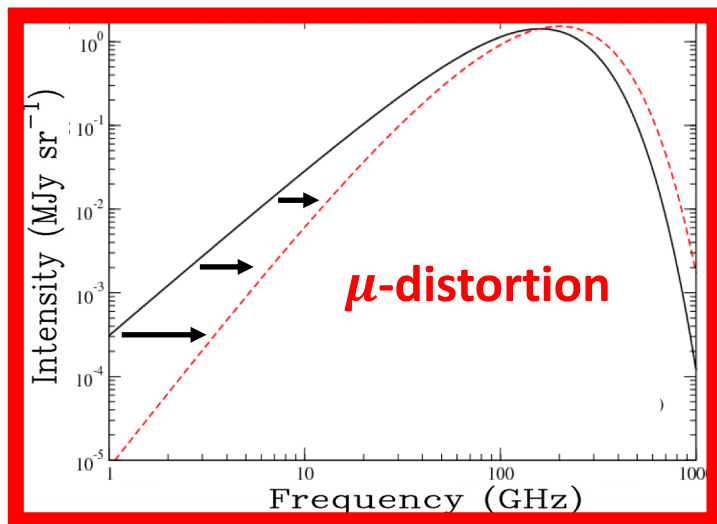


Zeldovich & Sunyaev, ApSS (1969)

CMB spectral distortions

Important at early times

$$z > 10^4$$



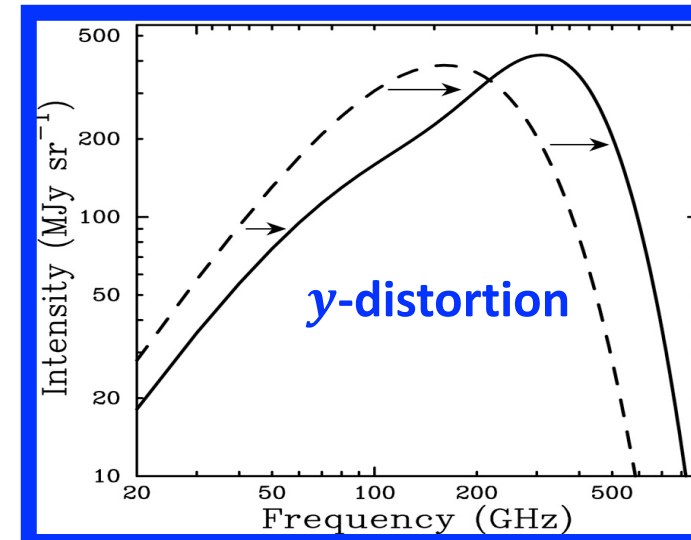
Sunyaev & Zeldovich, ApSS (1970)

$$I_\nu^{\text{CMB}} \simeq I_\nu^{\text{Planck}} \left(1 + \underbrace{\mu \frac{x e^x}{e^x - 1} \left[\frac{\pi^2}{18\zeta(3)} - \frac{1}{x} \right]}_{\text{spectral signature of } \mu\text{-distortion}} \right)$$

Blackbody

Important at late times

$$z < 10^4$$



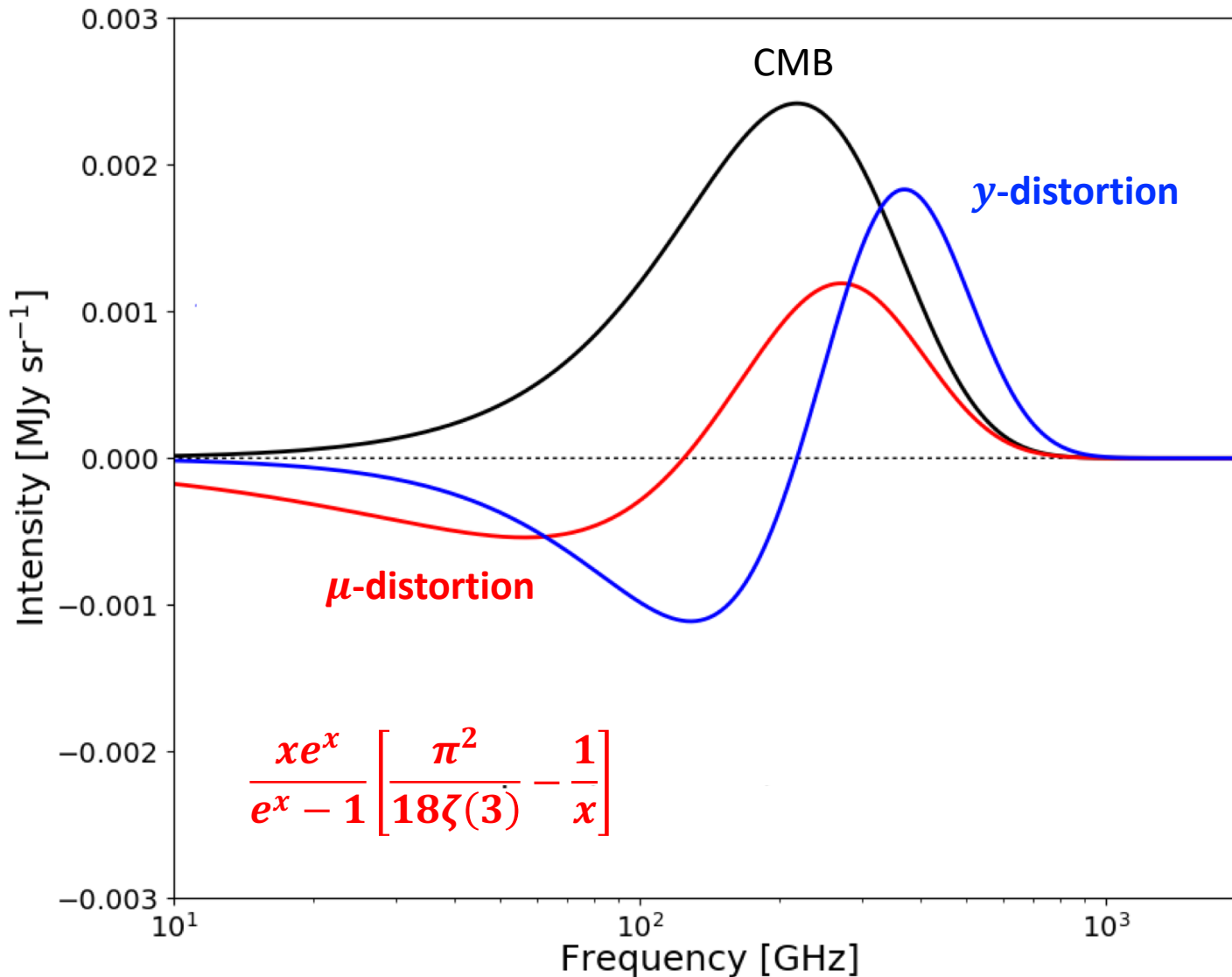
Zeldovich & Sunyaev, ApSS (1969)

$$I_\nu^{\text{CMB}} \simeq I_\nu^{\text{Planck}} \left(1 + \underbrace{y \frac{x e^x}{e^x - 1} \left[x \coth \frac{x}{2} - 4 \right]}_{\text{spectral signature of } y\text{-distortion}} \right)$$

Blackbody

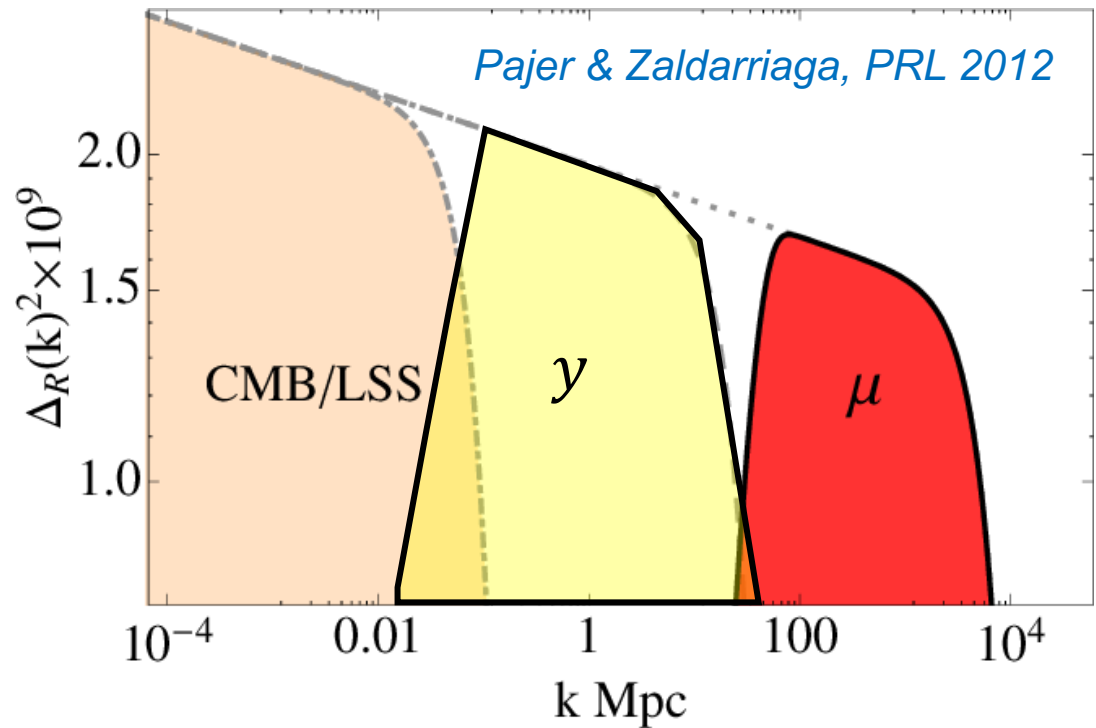
$$x \equiv h\nu/kT$$

Spectral shapes of distortions



$$\frac{xe^x}{e^x - 1} \left[x \coth \frac{x}{2} - 4 \right]$$

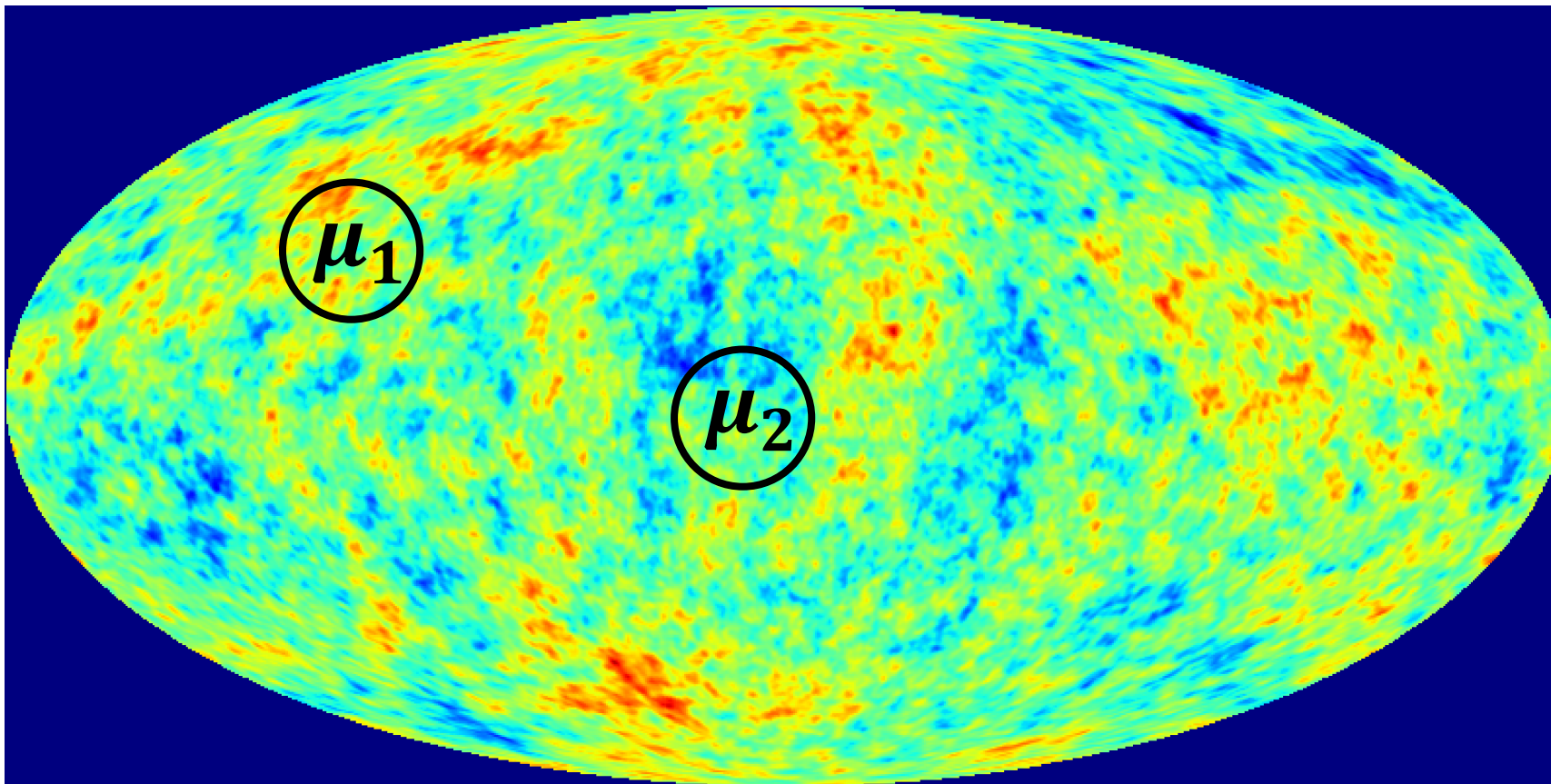
Spectral distortions probe the primordial power spectrum at very small scales



- CMB: $k > 0.2 \text{ Mpc}^{-1}$ erased by Silk damping
- LSS: $k > 0.2 \text{ Mpc}^{-1}$ very non-linear
- Spectral distortions extend our lever arm up to $k \simeq 10^3 \text{ Mpc}^{-1}$ in the linear regime!

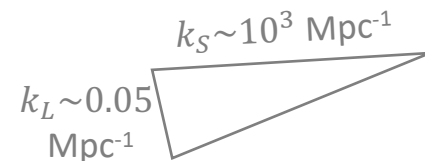
Aside from average distortions...

Anisotropies of spectral distortions from non-Gaussian primordial perturbations



Anisotropic distortions from non-Gaussianity

*Local type non-Gaussianity
“ultra squeezed”*



Pajer & Zaldarriaga, PRL 2012

- Multi-field inflation and non-Bunch-Davies vacuum models predict sizeable, scale-dependent, non-Gaussianity of the primordial perturbation field
- Non-gaussian couplings between short- and long-wavelength modes modulate the damping of primordial perturbations across different directions in the sky

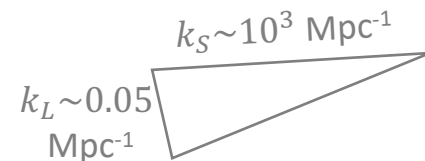
⇒ Anisotropic μ -distortions $\sim C_\ell^{\mu\mu}$

- Non-gaussian couplings ⇒ correlation between CMB temperature and μ -distortion anisotropies!

⇒ $C_\ell^{\mu T} \simeq f_{\text{NL}}(k \simeq 10^3 \text{ Mpc}^{-1}) \langle \mu \rangle \rho(\ell) C_\ell^{TT,SW}$

Anisotropic distortions from non-Gaussianity

Local type non-Gaussianity
“ultra squeezed”



Pajer & Zaldarriaga, PRL 2012

- Multi-field inflation and non-Bunch-Davies vacuum models predict sizeable, scale-dependent, non-Gaussianity of the primordial perturbation field
- Non-gaussian couplings between short- and long-wavelength modes modulate the damping of primordial perturbations across different directions in the sky

⇒ Anisotropic μ - and y -distortions $\sim C_\ell^{\mu\mu}, C_\ell^{yy}$

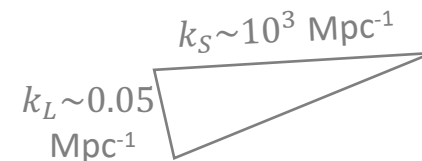
- Non-gaussian couplings ⇒ correlation between CMB temperature and μ -distortion anisotropies!

$$\Rightarrow C_\ell^{\mu T} \simeq f_{\text{NL}}(k \simeq 10^3 \text{ Mpc}^{-1}) \langle \mu \rangle \rho(\ell) C_\ell^{TT, \text{SW}}$$

$$\Rightarrow C_\ell^{yT} \simeq f_{\text{NL}}(k \simeq 10 \text{ Mpc}^{-1}) \langle y \rangle \tilde{\rho}(\ell) C_\ell^{TT, \text{SW}}$$

Anisotropic distortions from non-Gaussianity

Local type non-Gaussianity
“ultra squeezed”



Pajer & Zaldarriaga, PRL 2012

- Multi-field inflation and non-Bunch-Davies vacuum models predict sizeable, scale-dependent, non-Gaussianity of the primordial perturbation field
- Non-gaussian couplings between short- and long-wavelength modes modulate the damping of primordial perturbations across different directions in the sky

⇒ Anisotropic μ - and y -distortions $\sim C_\ell^{\mu\mu}, C_\ell^{yy}$

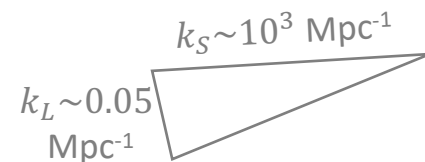
- Non-gaussian couplings ⇒ correlation between CMB temperature and μ -distortion anisotropies!

$$\left[\begin{array}{l} \Rightarrow C_\ell^{\mu T} \simeq f_{\text{NL}}(k \simeq 10^3 \text{ Mpc}^{-1}) \langle \mu \rangle \rho(\ell) C_\ell^{TT, \text{SW}} \\ \Rightarrow C_\ell^{yT} \simeq f_{\text{NL}}(k \simeq 10 \text{ Mpc}^{-1}) \langle y \rangle \tilde{\rho}(\ell) C_\ell^{TT, \text{SW}} \end{array} \right]$$

Enhanced distortion signals by cross-correlation with CMB temperature anisotropies!

Anisotropic distortions from non-Gaussianity

Local type non-Gaussianity
“ultra squeezed”



Pajer & Zaldarriaga, PRL 2012

- Multi-field inflation and non-Bunch-Davies vacuum models predict sizeable, scale-dependent, non-Gaussianity of the primordial perturbation field
- Non-gaussian couplings between short- and long-wavelength modes modulate the damping of primordial perturbations across different directions in the sky

⇒ Anisotropic μ - and y -distortions $\sim C_\ell^{\mu\mu}, C_\ell^{yy}$

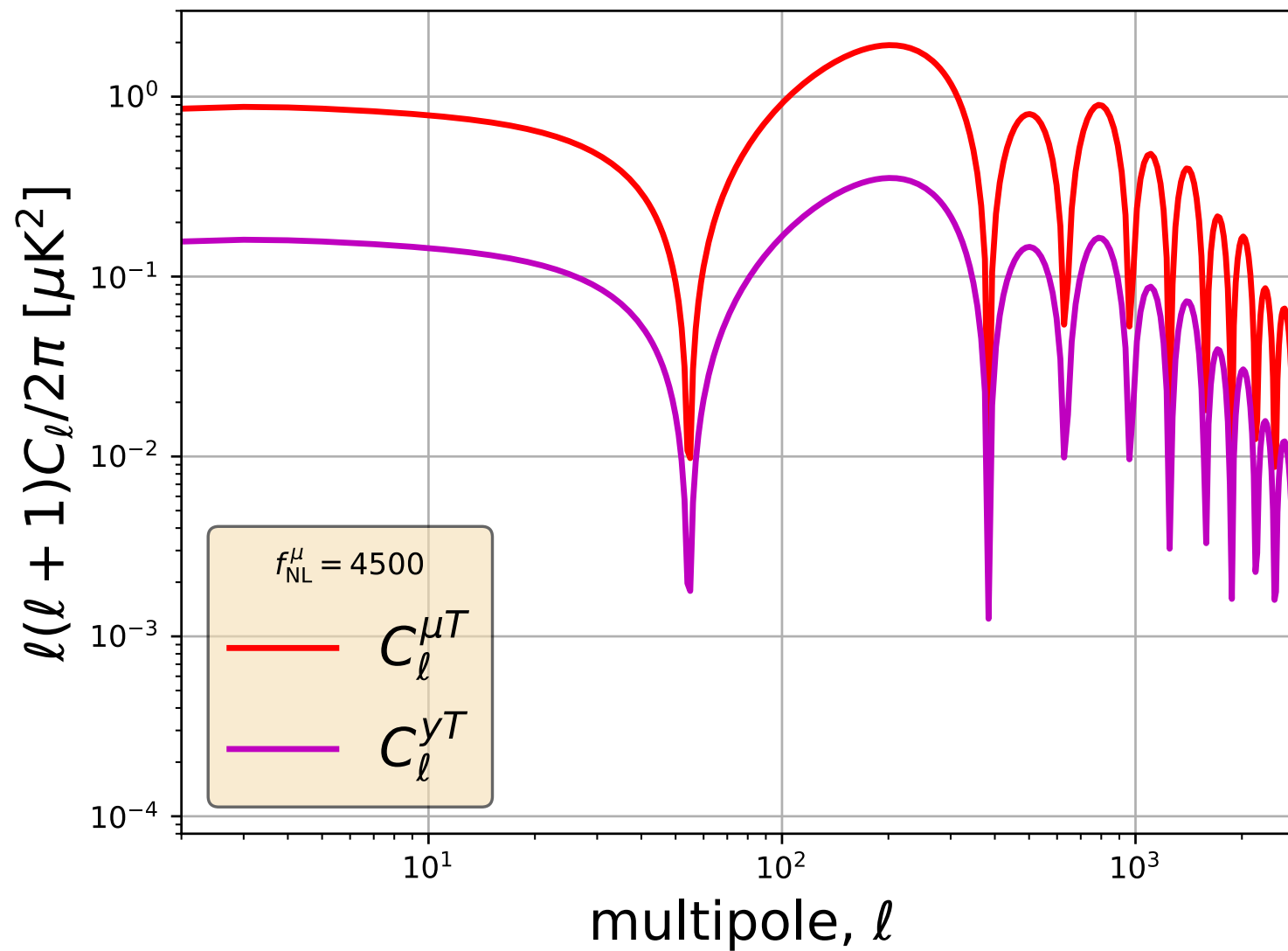
- Non-gaussian couplings ⇒ correlation between CMB temperature and μ -distortion anisotropies!

$$\Rightarrow C_\ell^{\mu T} \simeq f_{\text{NL}}(k \simeq 10^3 \text{ Mpc}^{-1}) \langle \mu \rangle \rho(\ell) C_\ell^{TT, \text{SW}}$$

$$\Rightarrow C_\ell^{yT} \simeq f_{\text{NL}}(k \simeq 10 \text{ Mpc}^{-1}) \langle y \rangle \tilde{\rho}(\ell) C_\ell^{TT, \text{SW}}$$

New pivot scales to probe the scale-dependence of primordial non-Gaussianity!

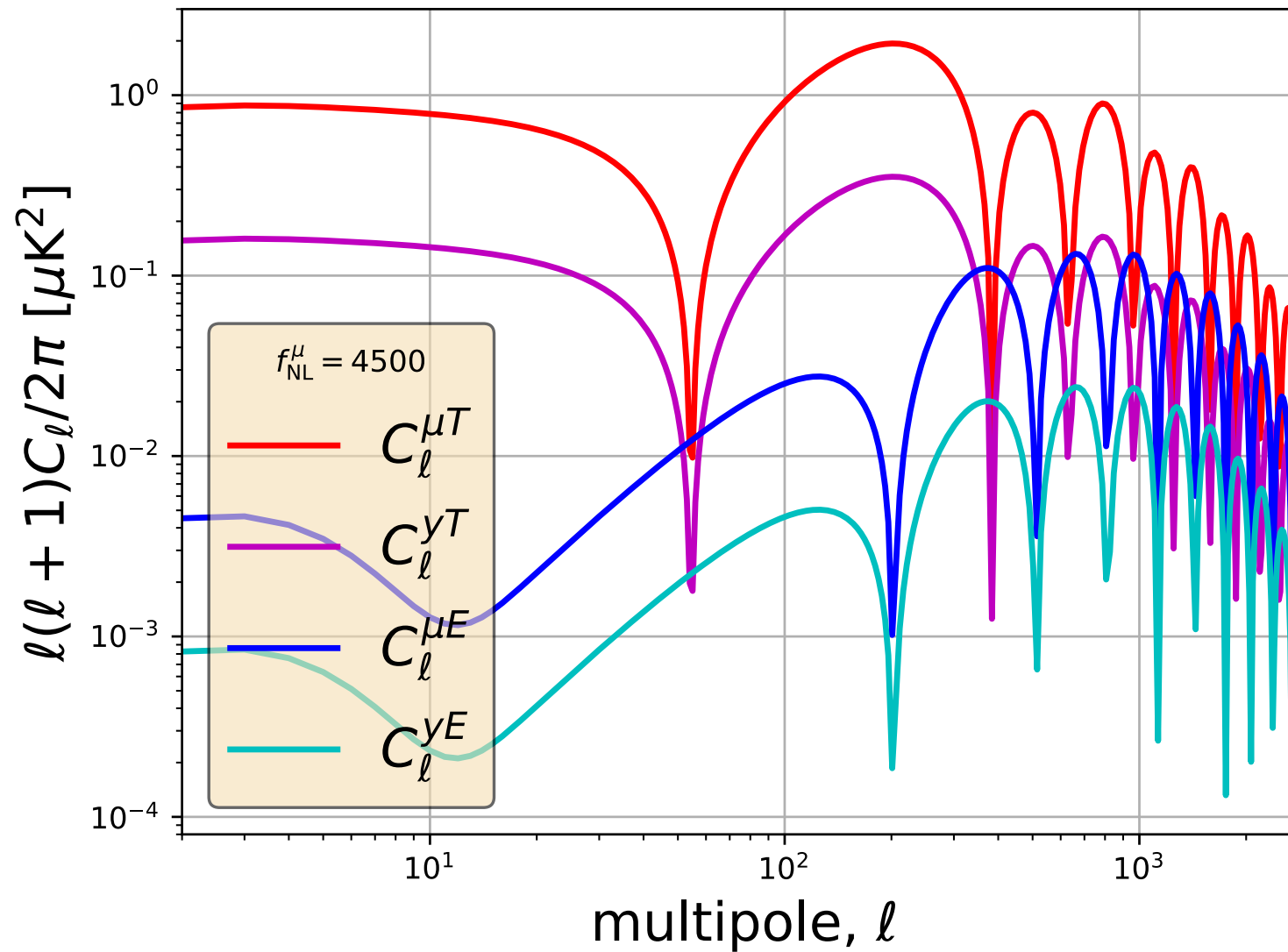
Theory



Ravenni et al
JCAP 2017

CMB polarization adds more leverage!

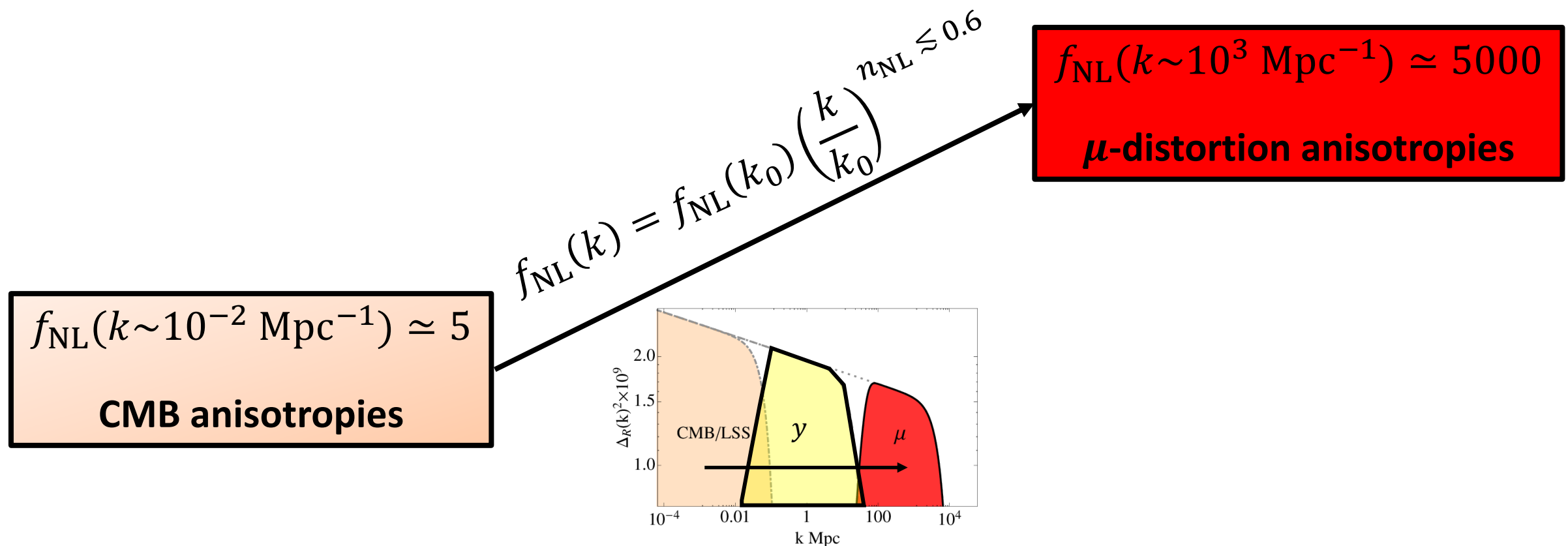
Ravenni et al
JCAP 2017



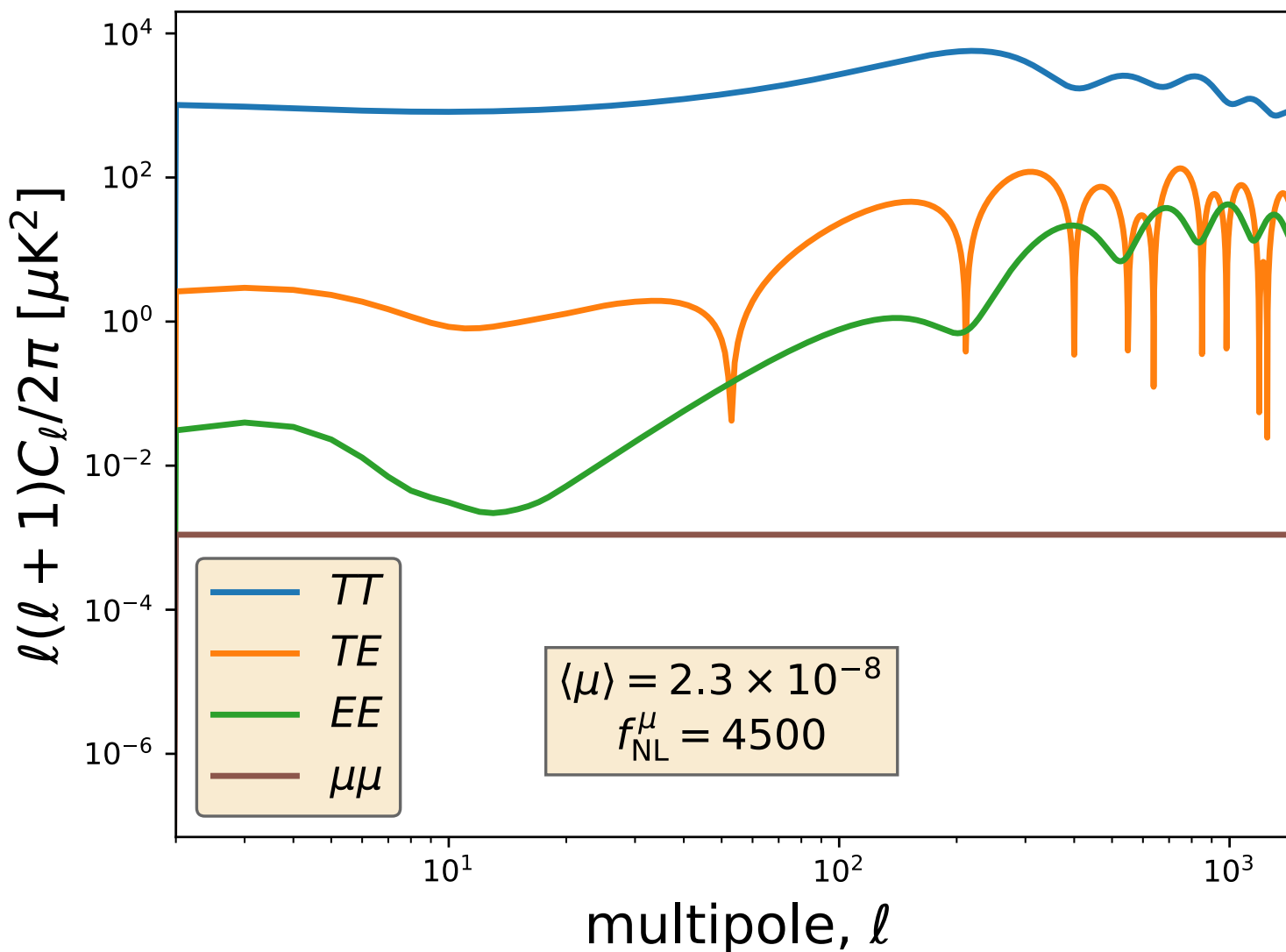
Extra bits
of information
from μE , $y E$
correlations!

Huge dynamic range of scales between CMB and μ -distortion probes

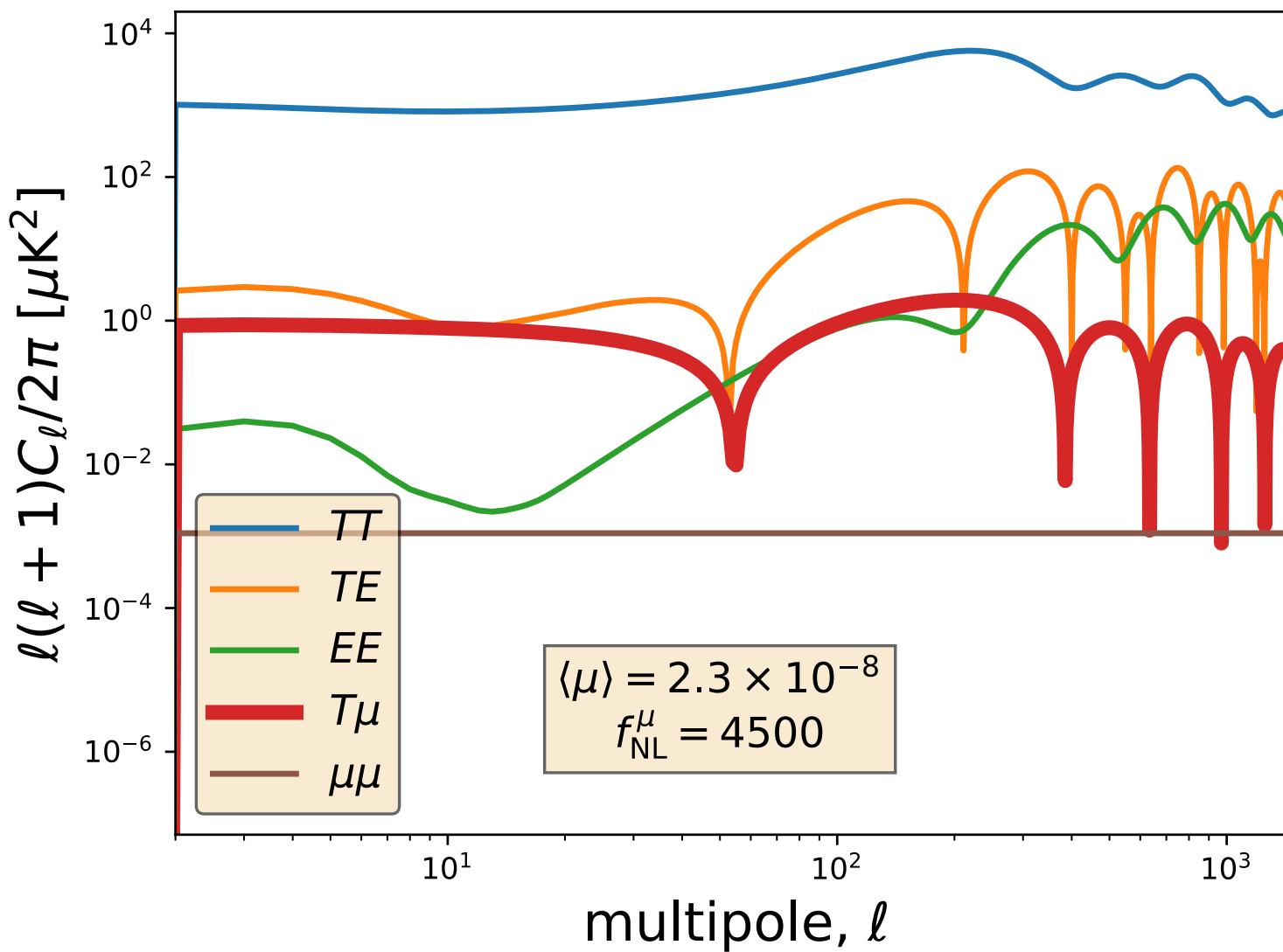
→ Mild scale dependence allows for large f_{NL} values at large wavenumber k



Orders of magnitude

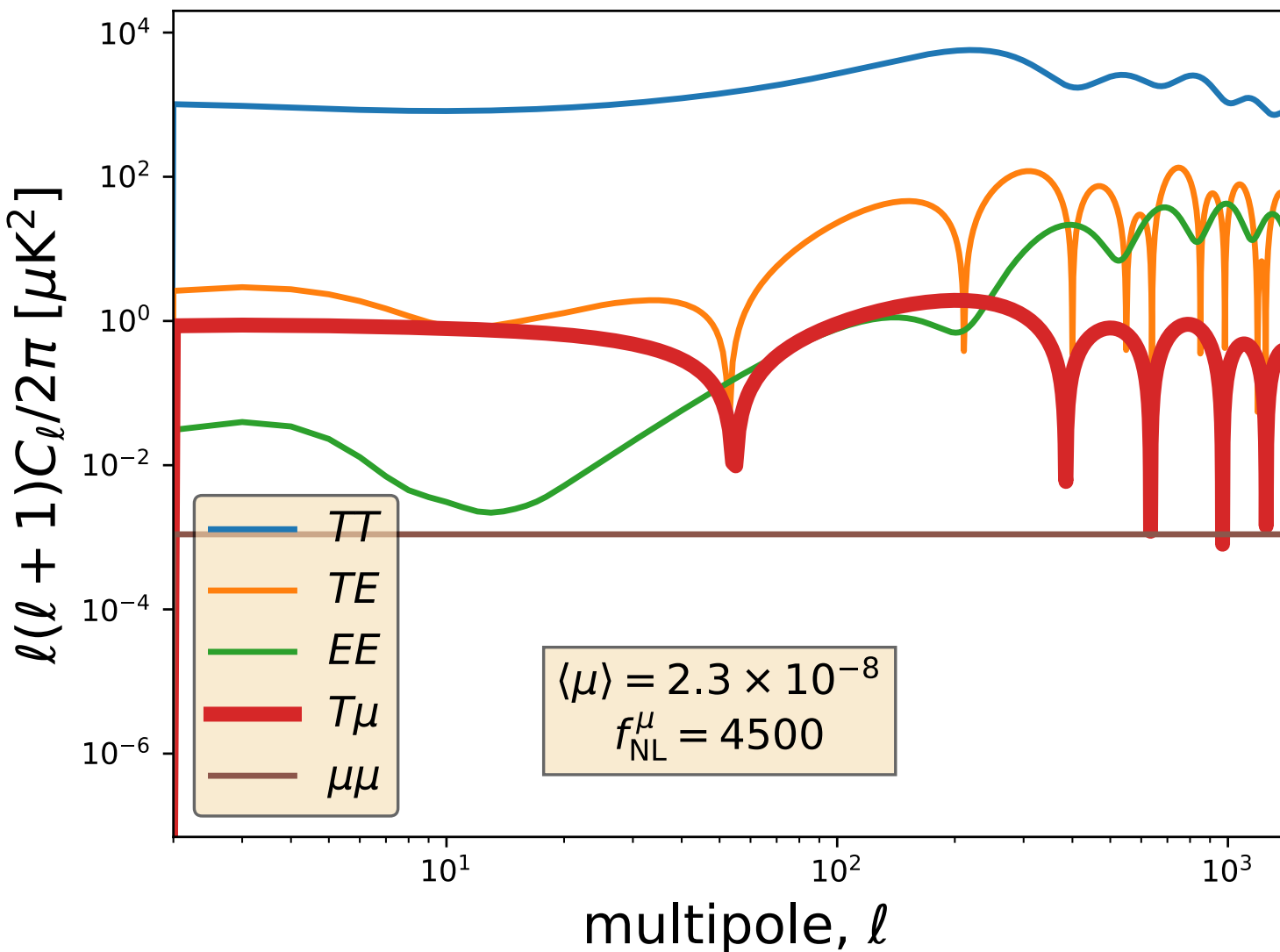


Orders of magnitude



For $f_{NL}^\mu \simeq 4500$
 μT comparable
to TE and EE

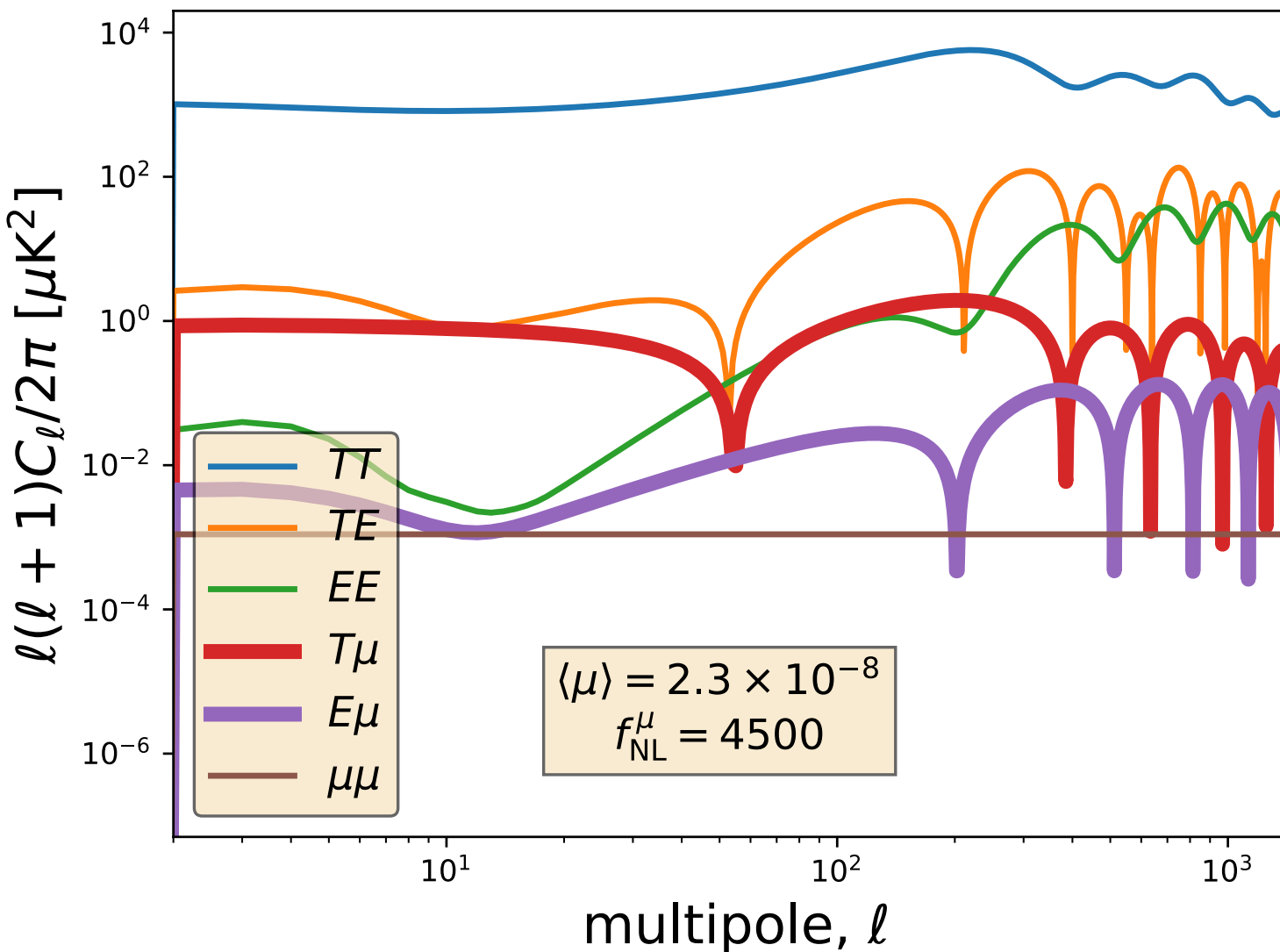
Orders of magnitude



For $f_{\text{NL}}^\mu \simeq 4500$
 μT comparable
to TE and EE

A science case
for future
CMB imagers!

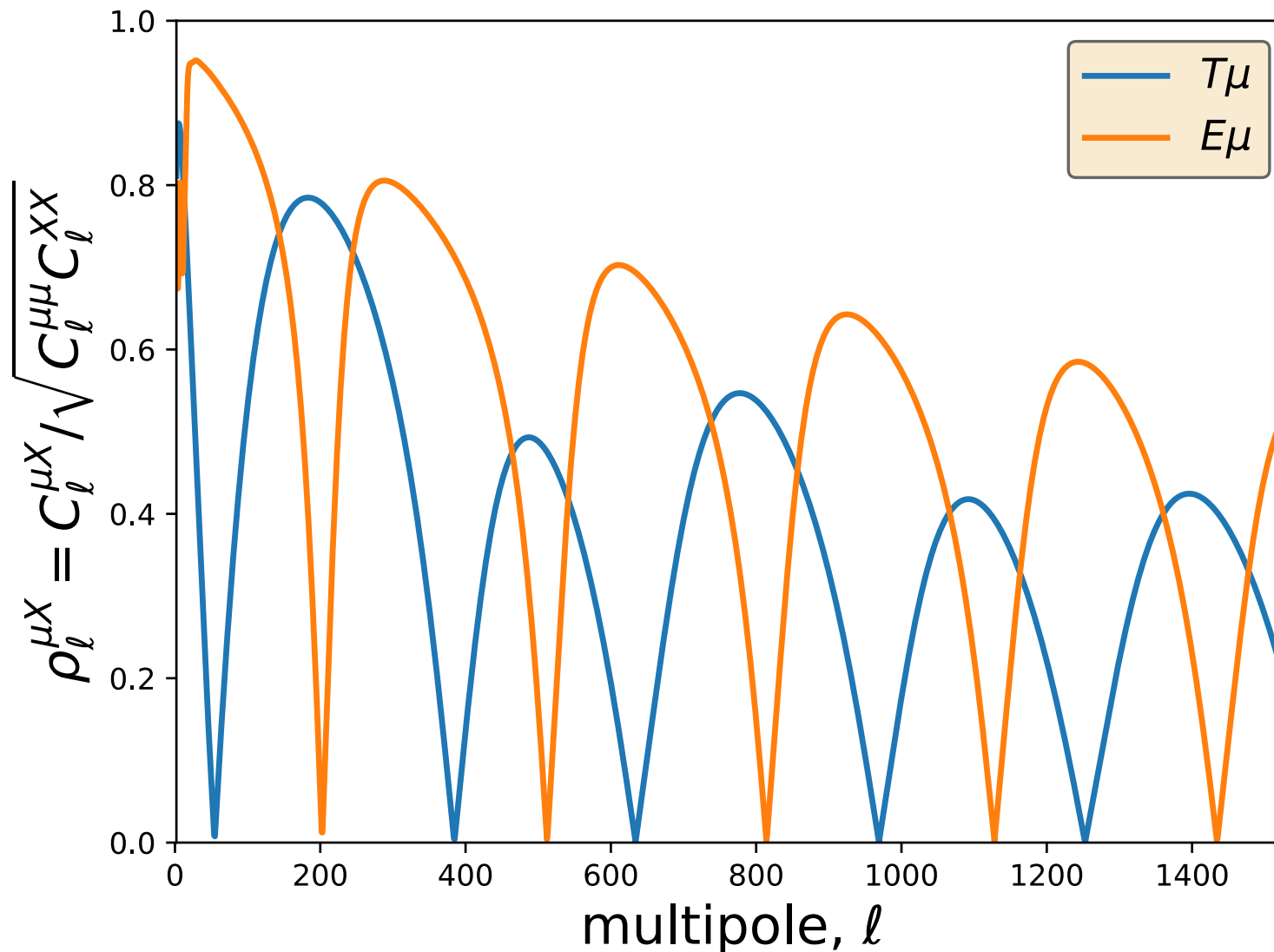
Orders of magnitude



$\mu E / EE$ ratio
larger than
 $\mu T / TT$ ratio

A science case
for future
CMB imagers!

Degree of correlation: $\mu \times E$ vs $\mu \times T$

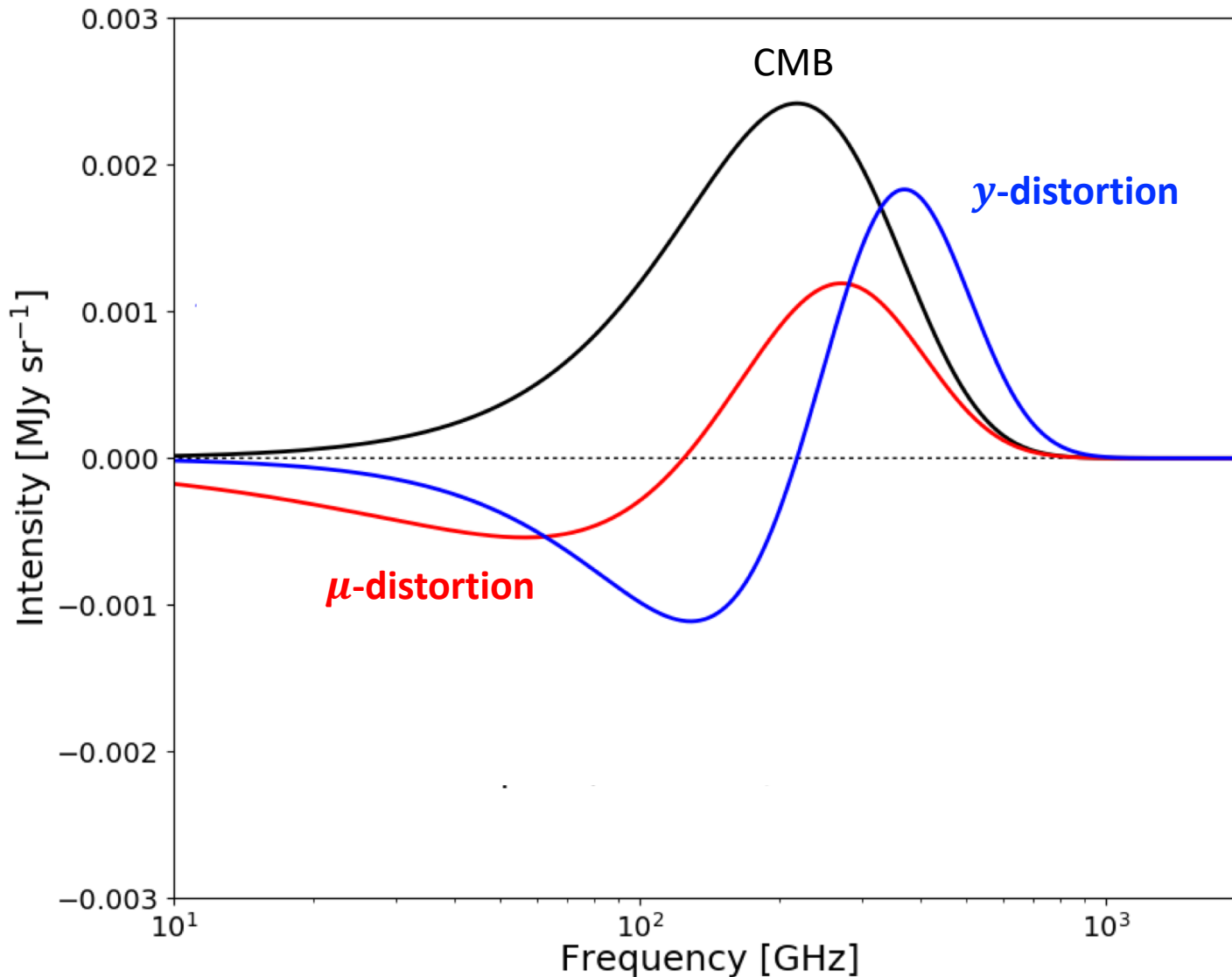


μE correlation
larger than
 μT correlation!

Questions

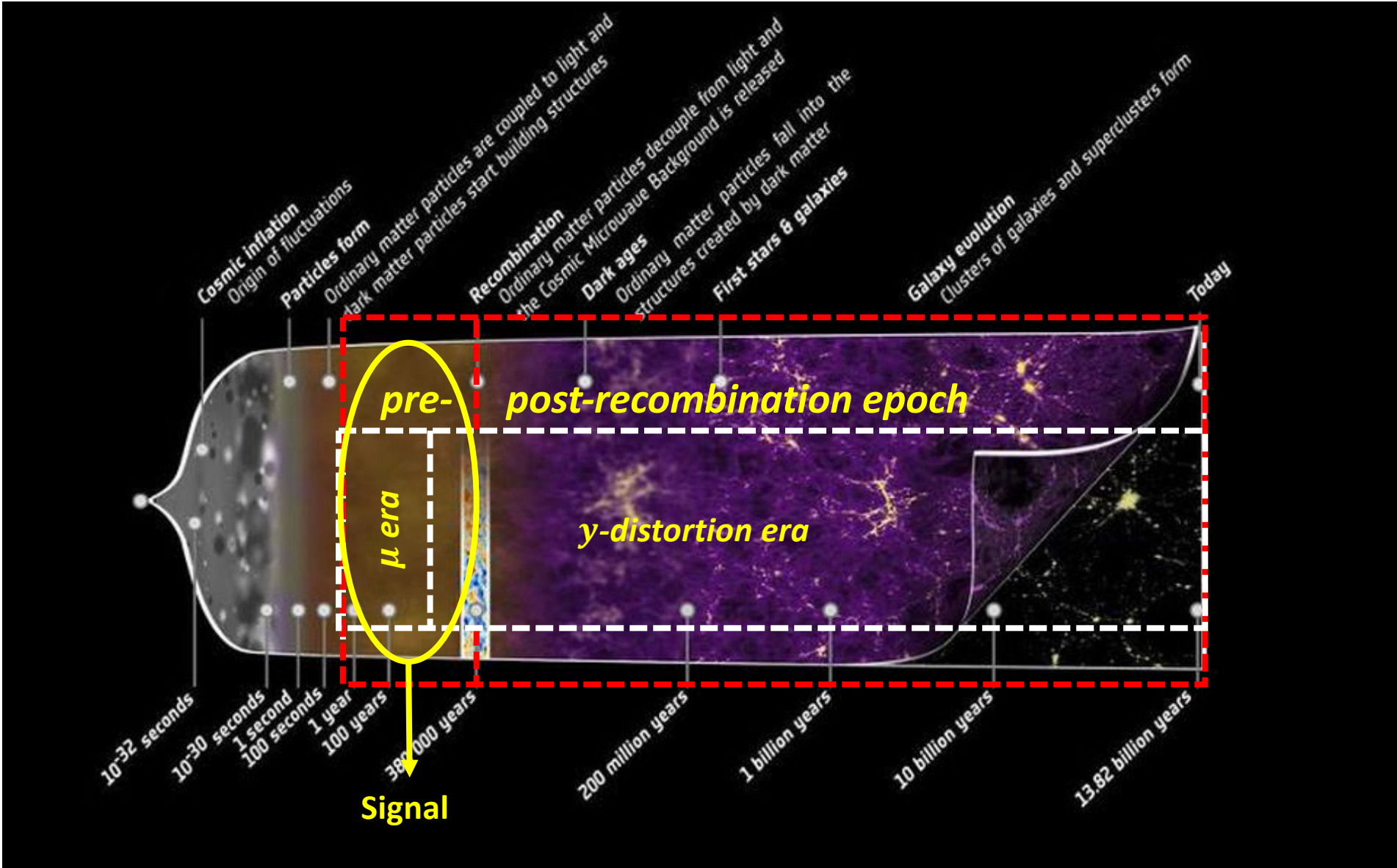
- ❑ Can we detect μT and μE correlated anisotropies with a future CMB satellite like *LiteBIRD*?
- ❑ What constraints on $f_{\text{NL}}^{\mu}(k \simeq 740 \text{ Mpc}^{-1})$ can be achieved with *LiteBIRD* in the presence of foregrounds?
- ❑ How much do we gain on f_{NL} sensitivity by including cross-correlations with CMB E -mode polarization?

Distinct spectral signatures of distortions

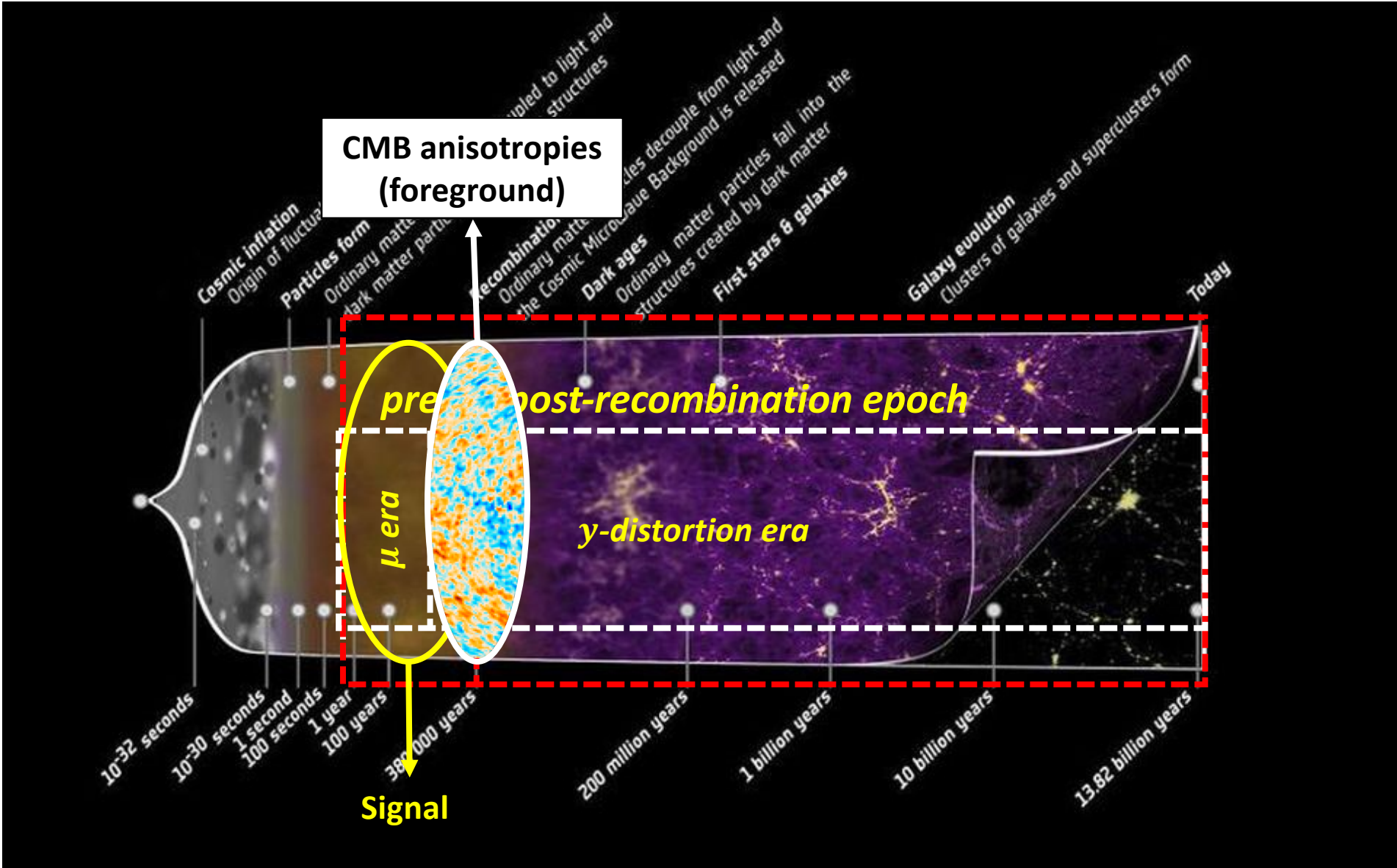


Multi-frequency observations can help us to disentangle them!

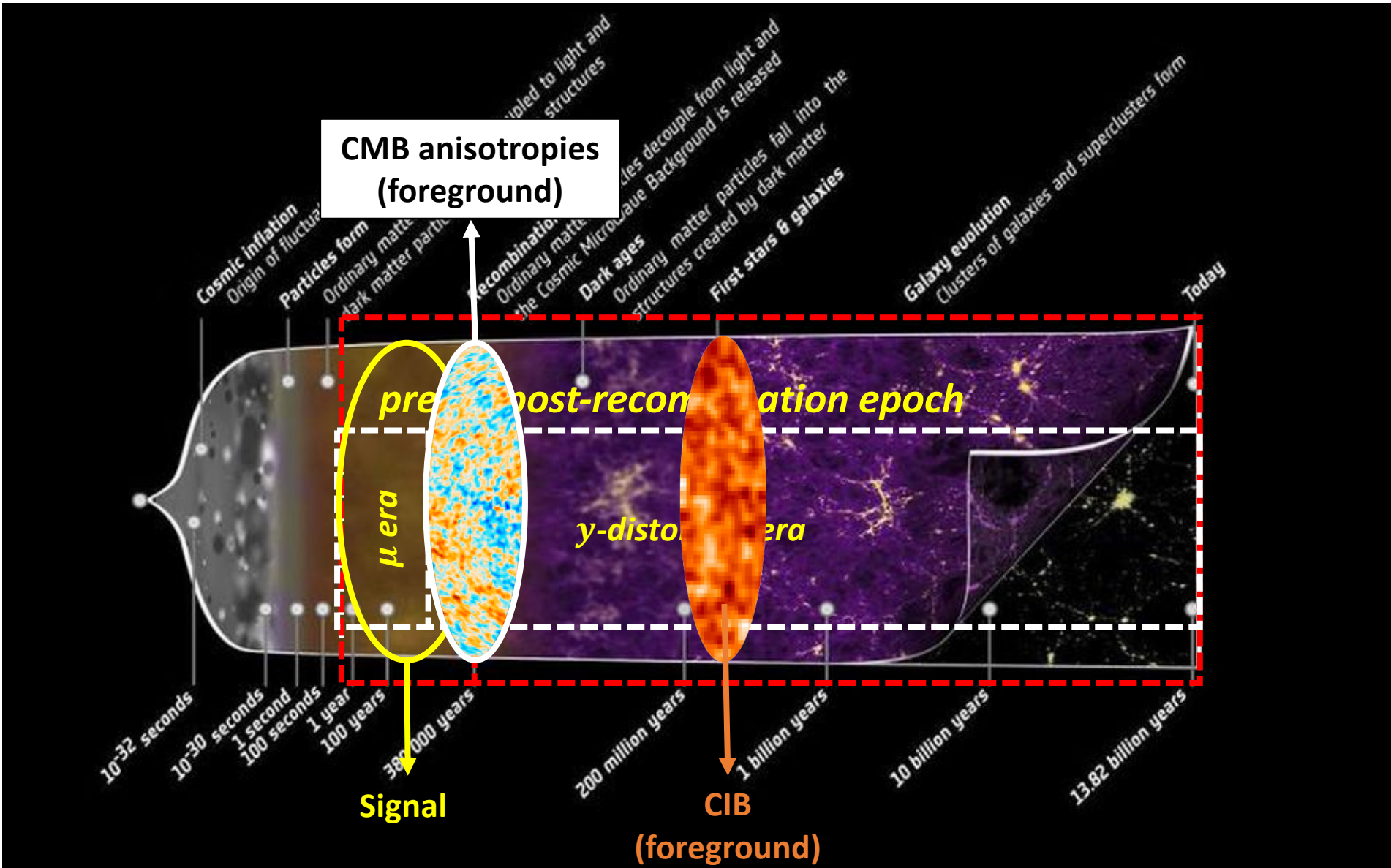
Foregrounds obscure SD anisotropies



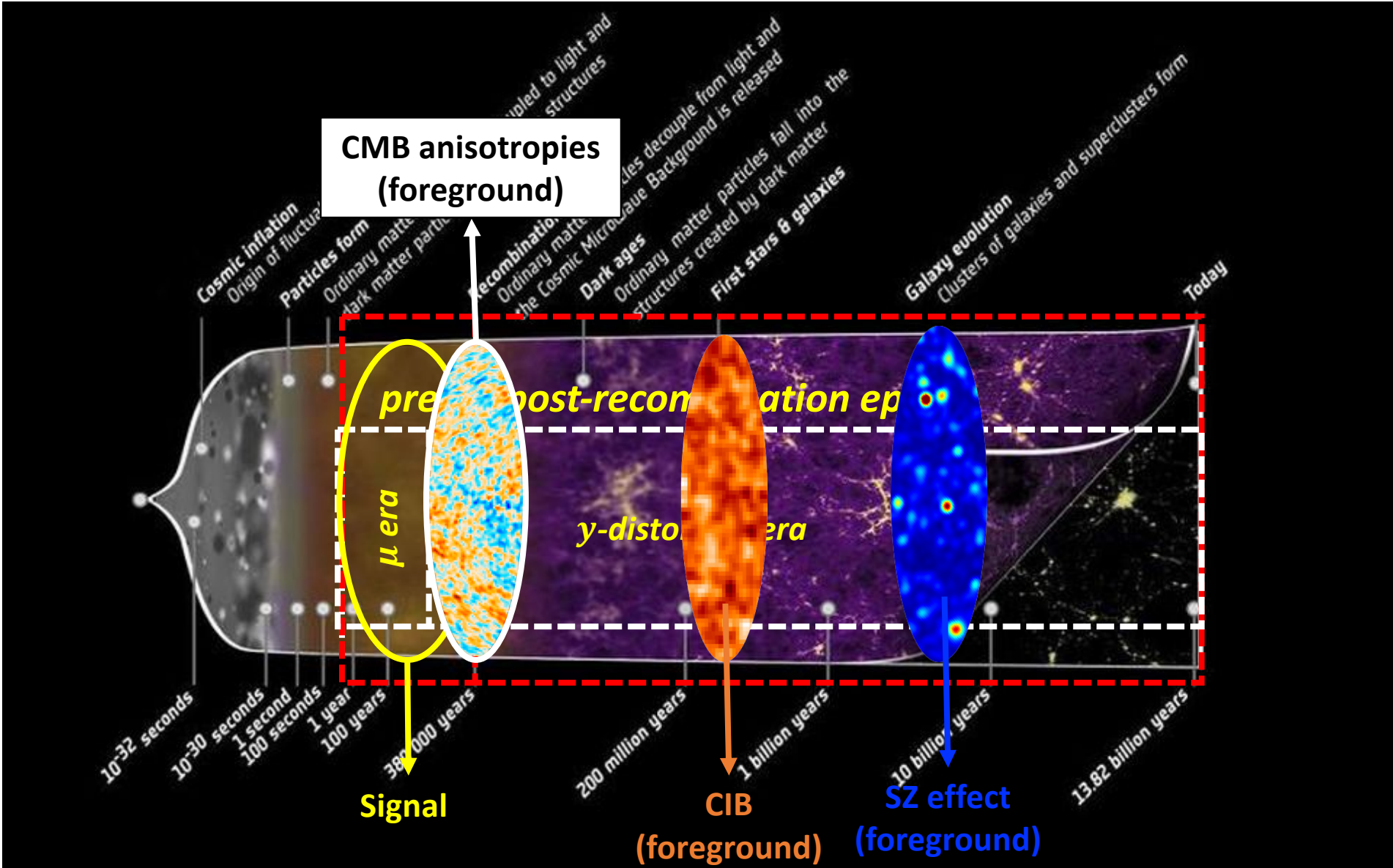
Foregrounds obscure SD anisotropies



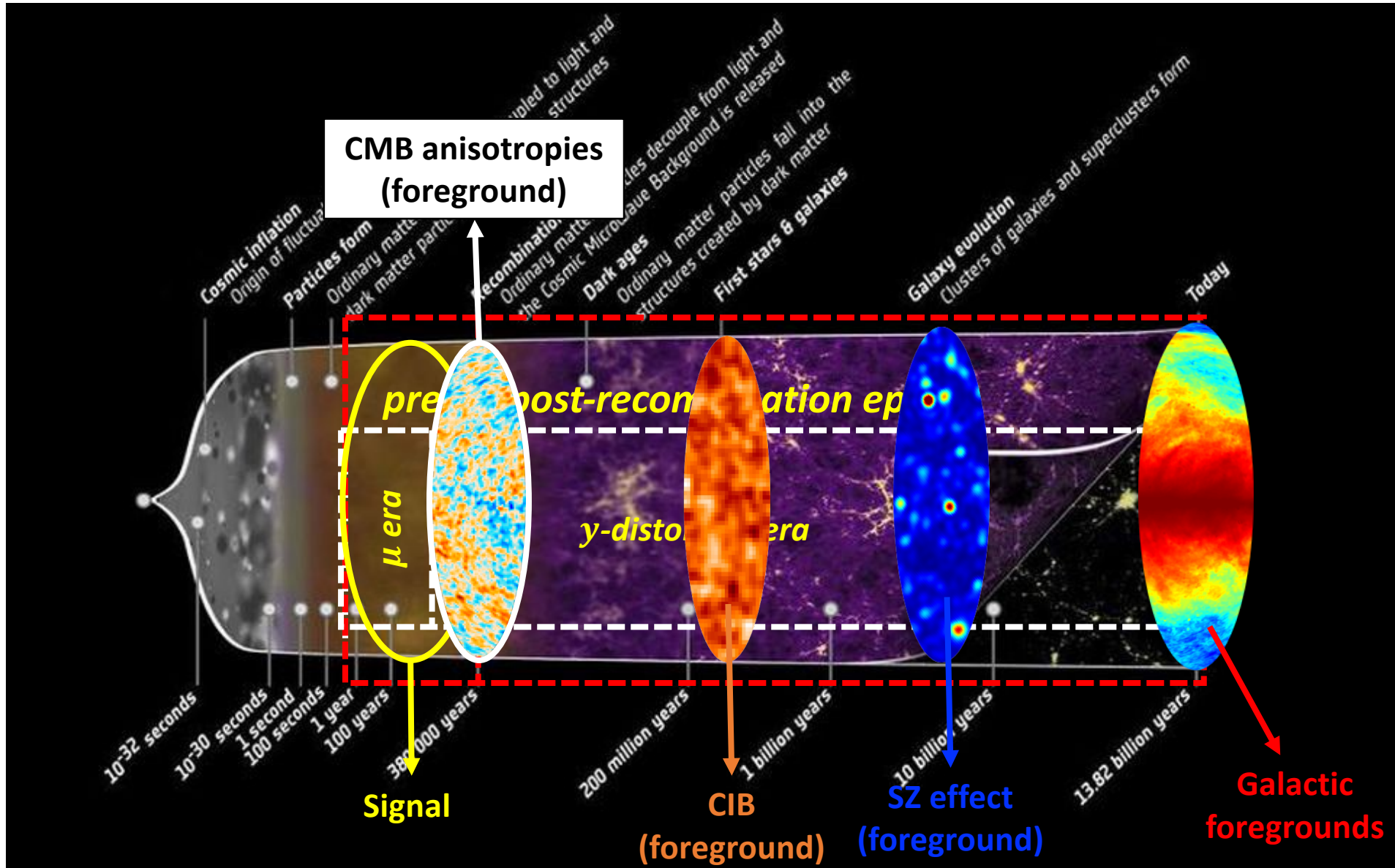
Foregrounds obscure SD anisotropies



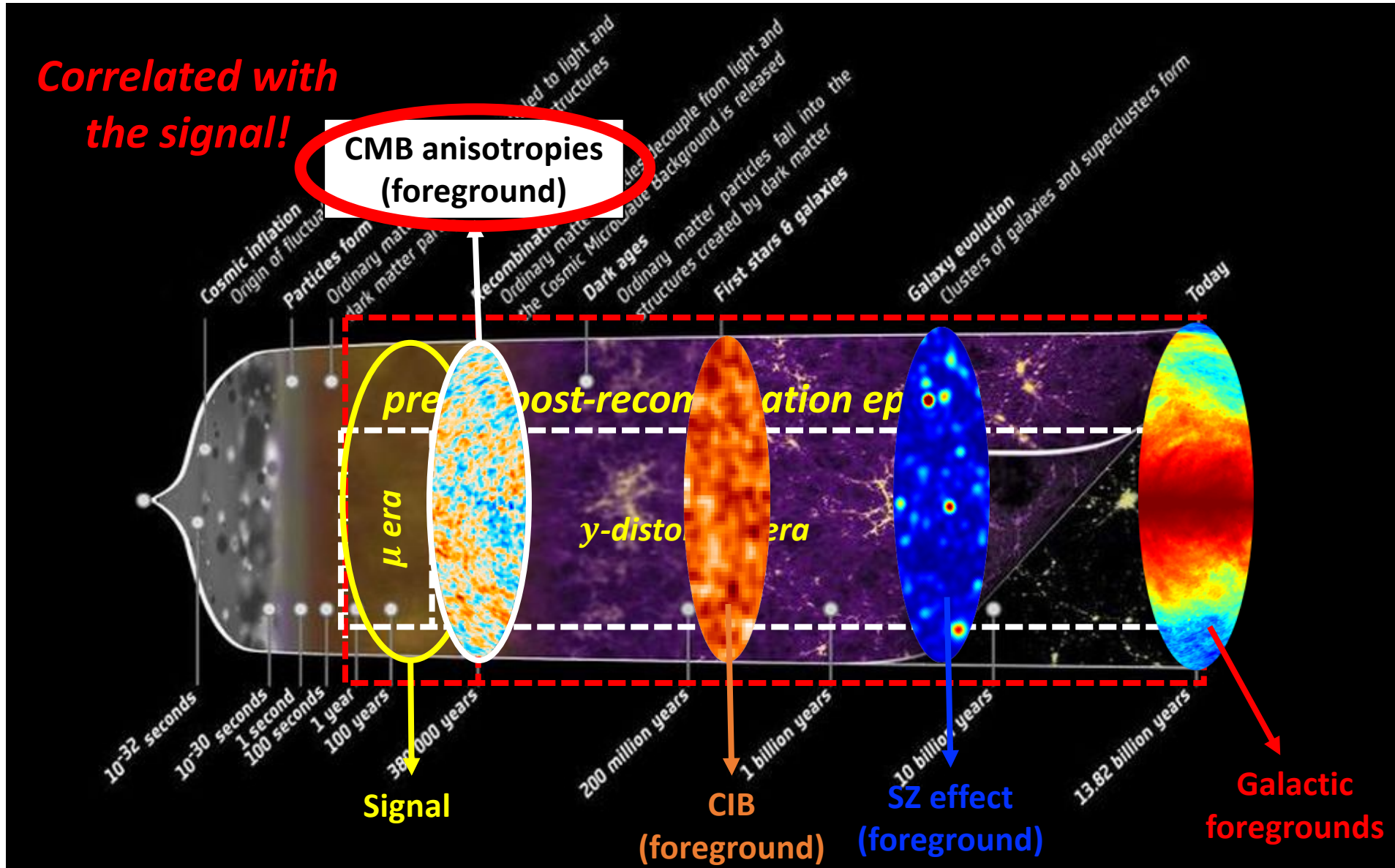
Foregrounds obscure SD anisotropies



Foregrounds obscure SD anisotropies

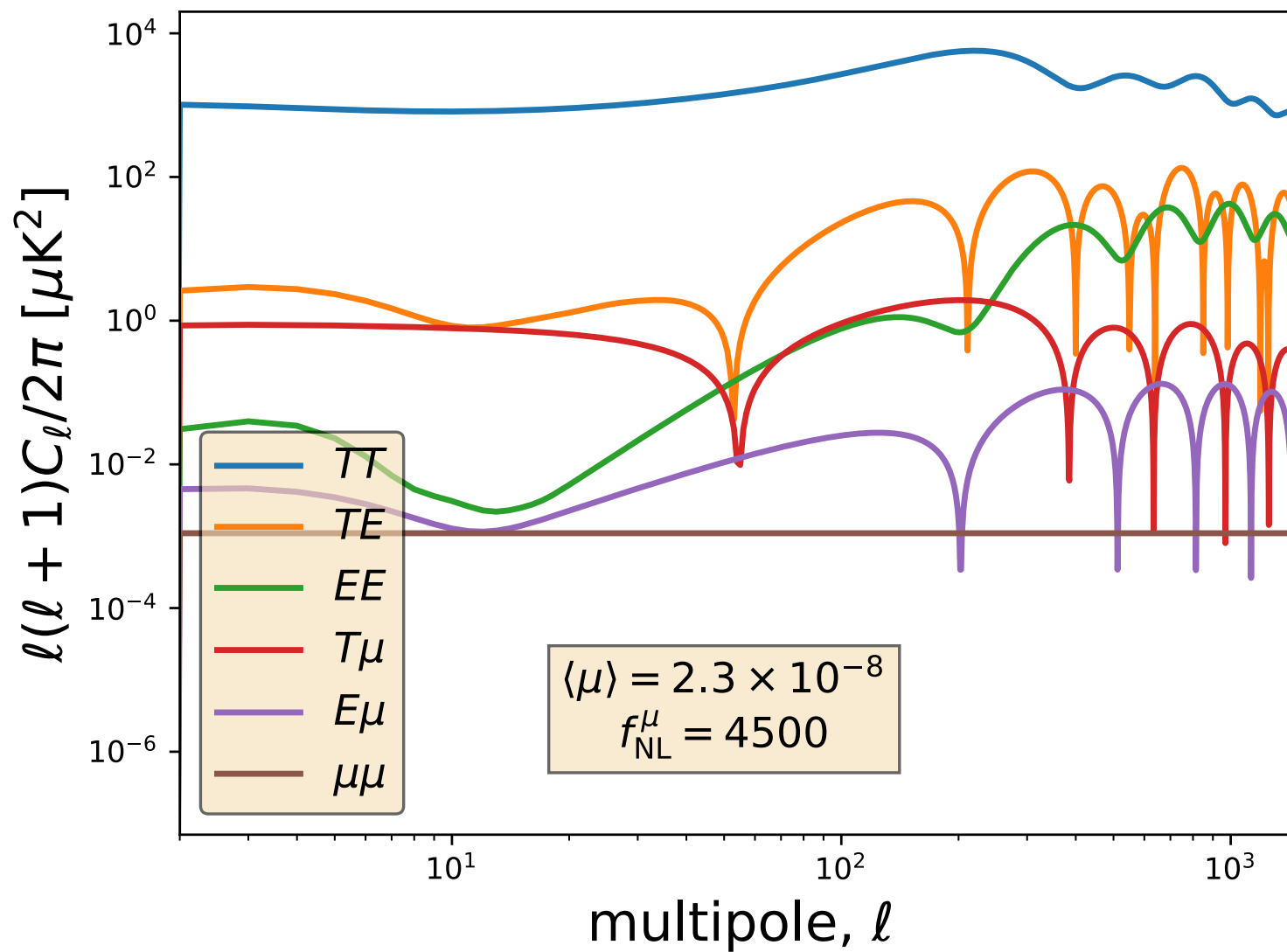


Foregrounds obscure SD anisotropies



Analysis

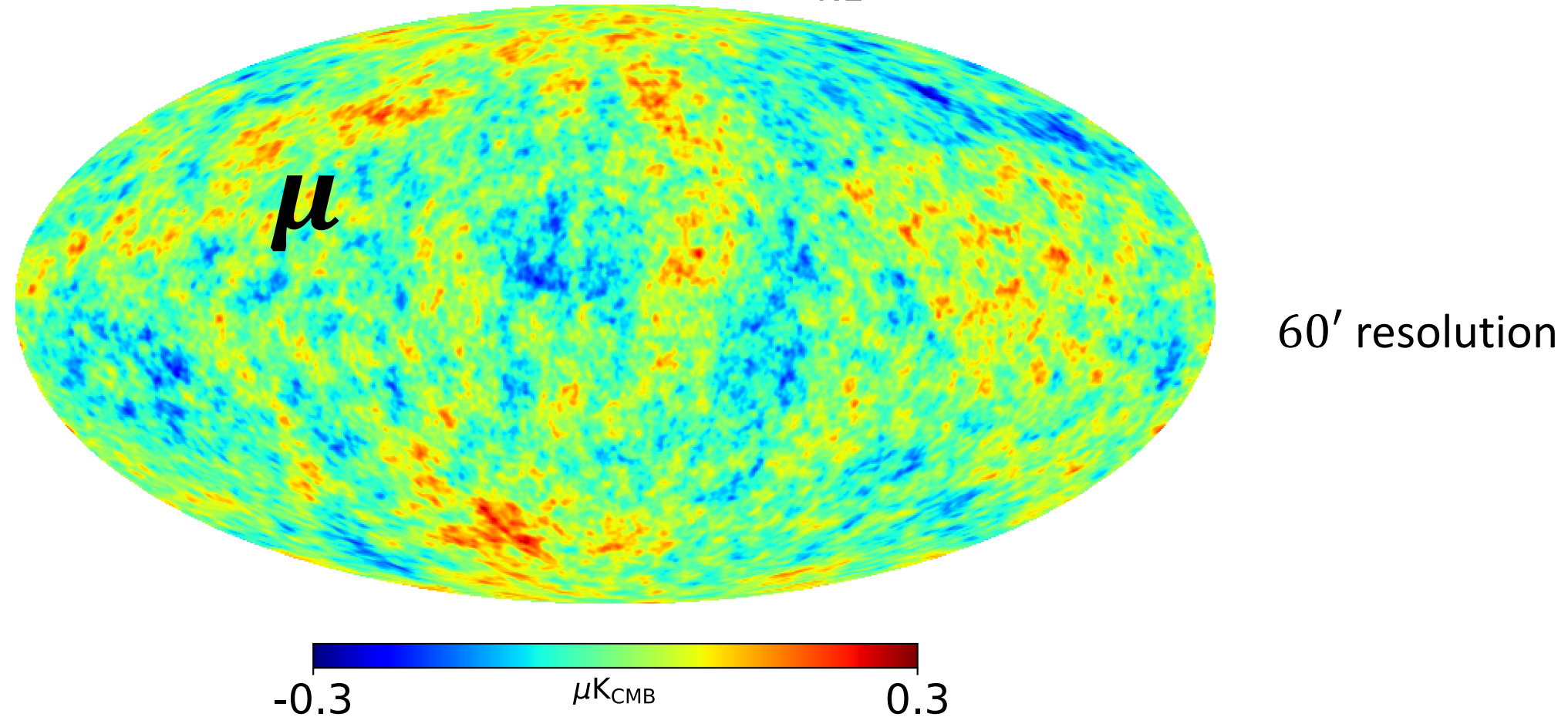
Theory



Ravenni et al
JCAP 2017

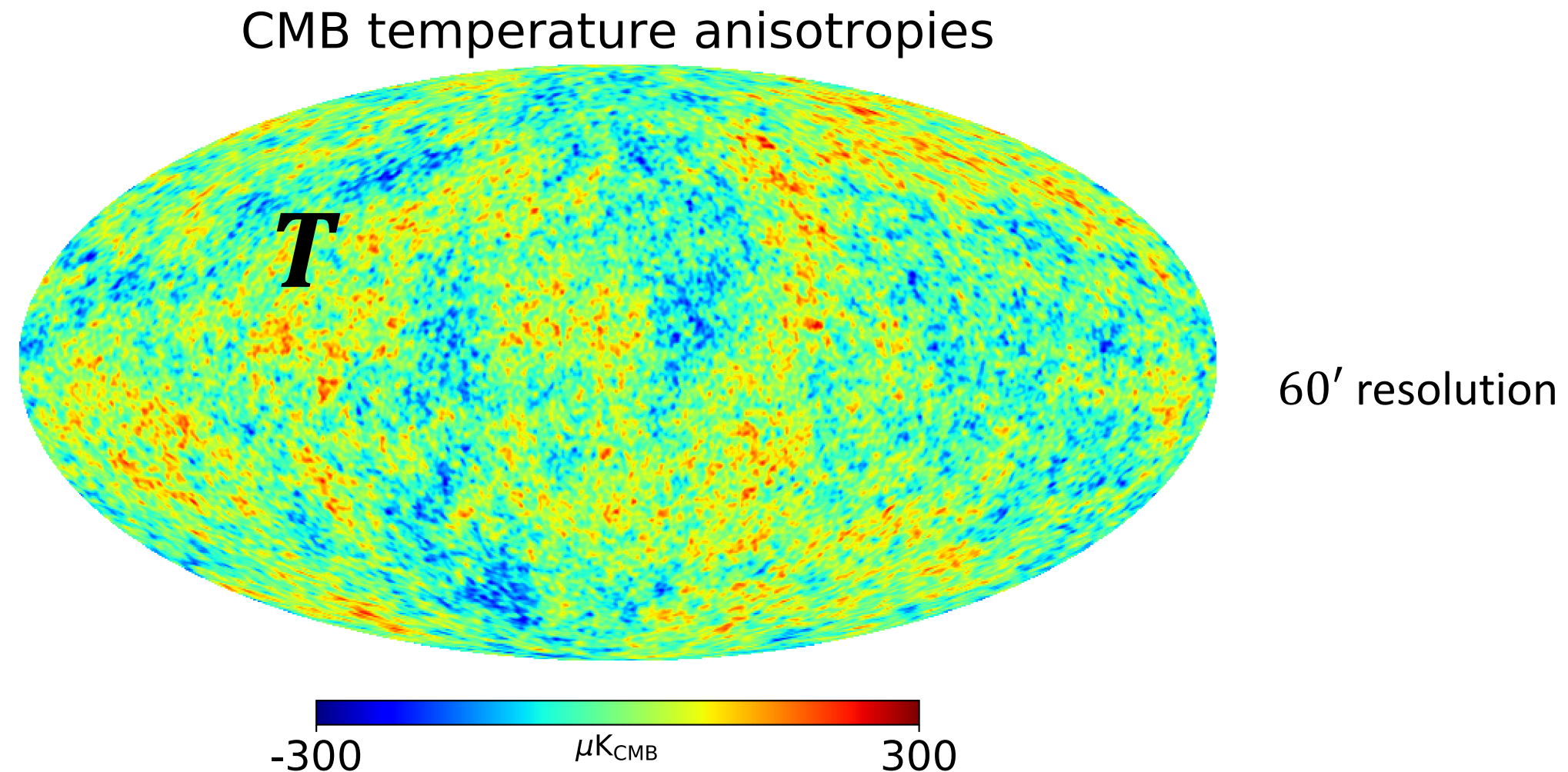
Correlated map simulations using Cholesky

μ -distortion anisotropies ($f_{\text{NL}}^{\mu} = 4500$)



Remazeilles, Ravenni, Chluba (2110.14664)

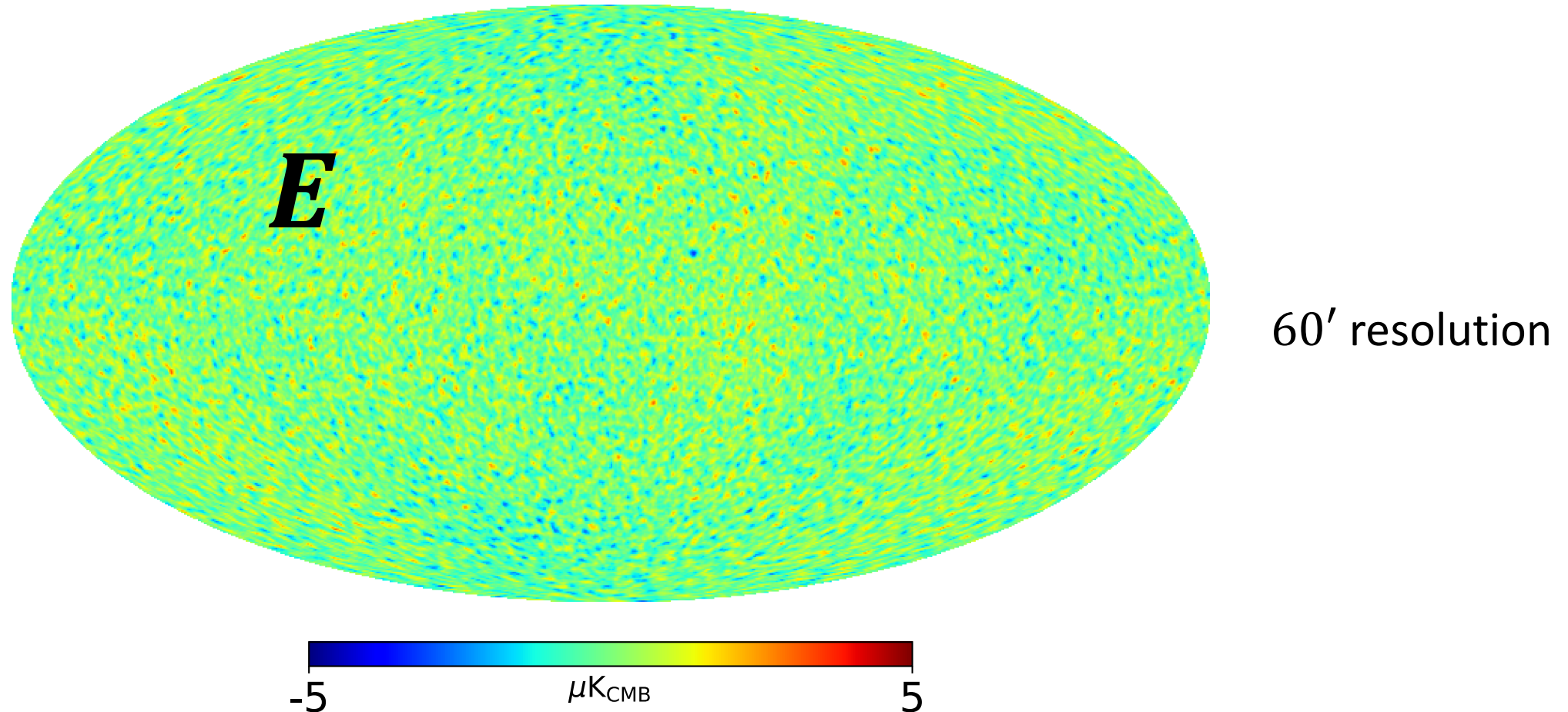
Correlated map simulations using Cholesky



Remazeilles, Ravenni, Chluba (2110.14664)

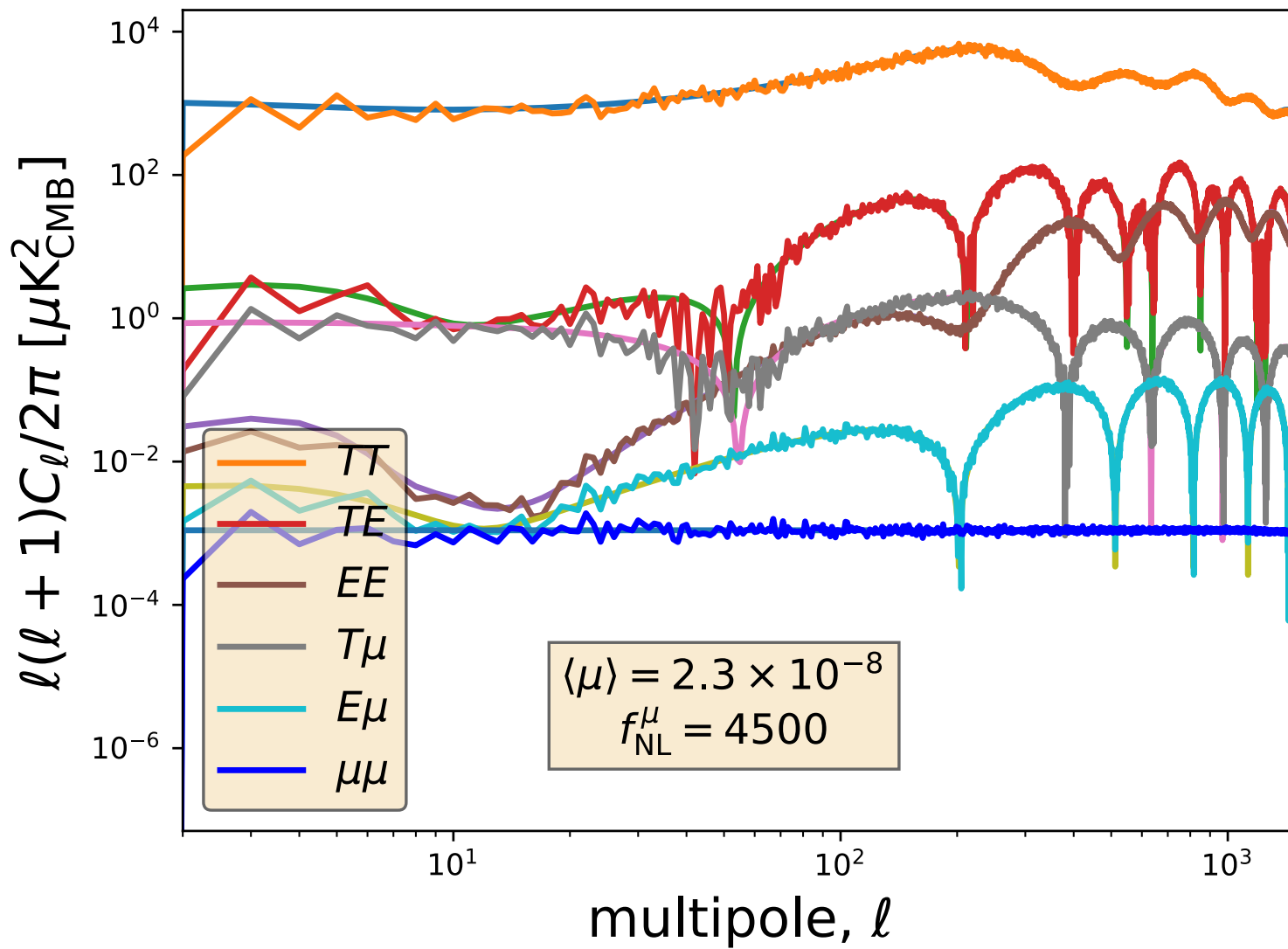
Correlated map simulations using Cholesky

CMB E-mode polarization anisotropies



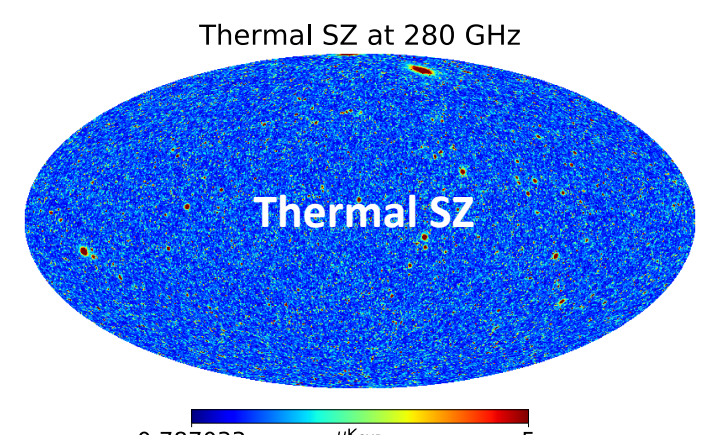
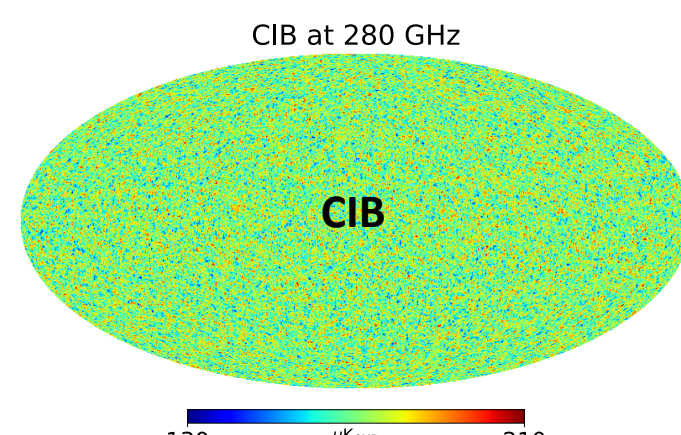
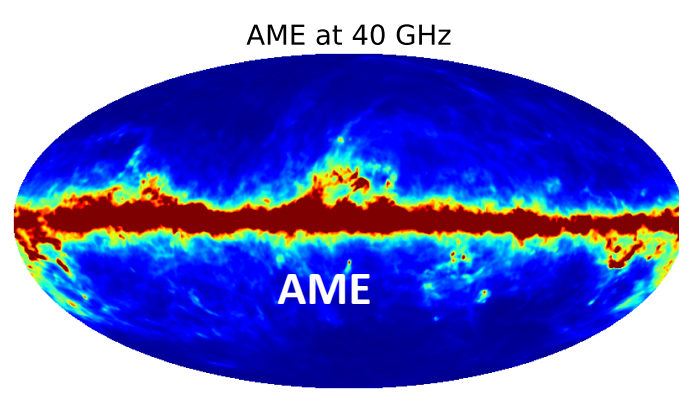
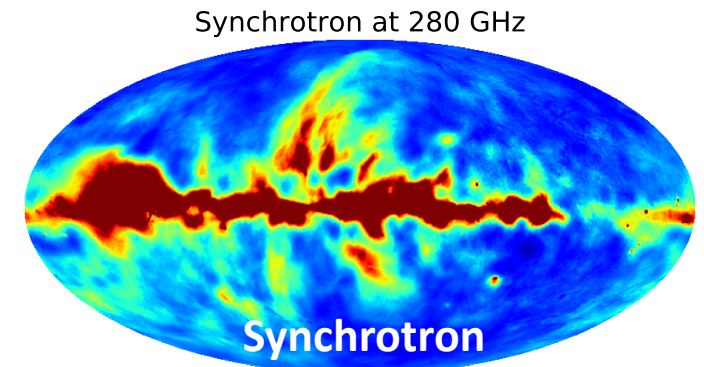
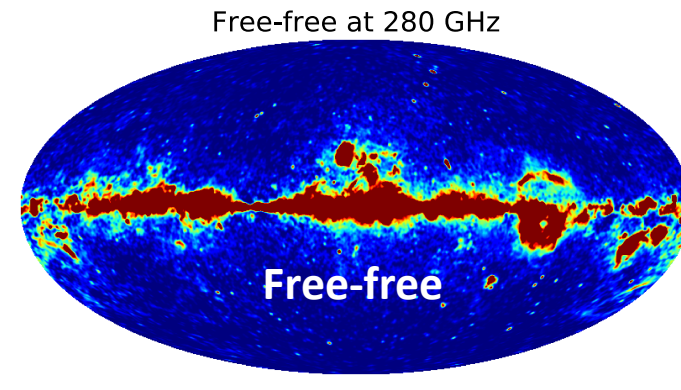
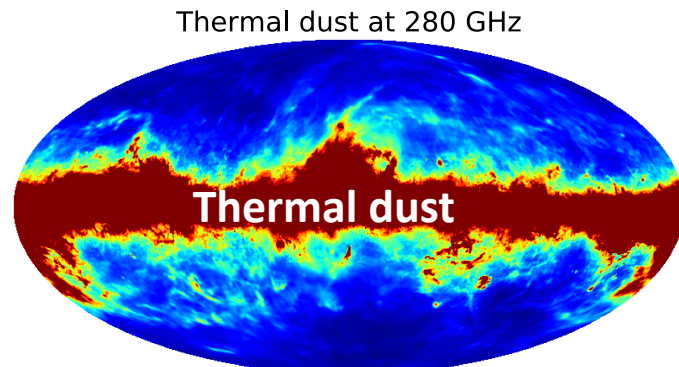
Remazeilles, Ravenni, Chluba (2110.14664)

Correlated map simulations using Cholesky



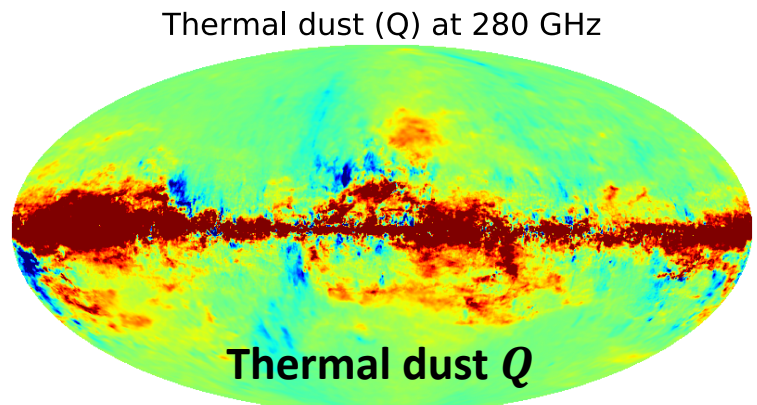
Remazeilles,
Ravenni,Chluba
2110.14664

Foregrounds simulation (temperature)

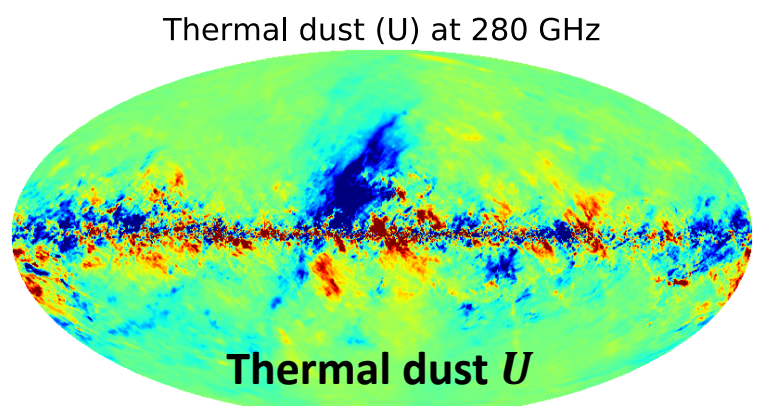


*Remazeilles, Ravenni, Chluba
(2110.14664)*

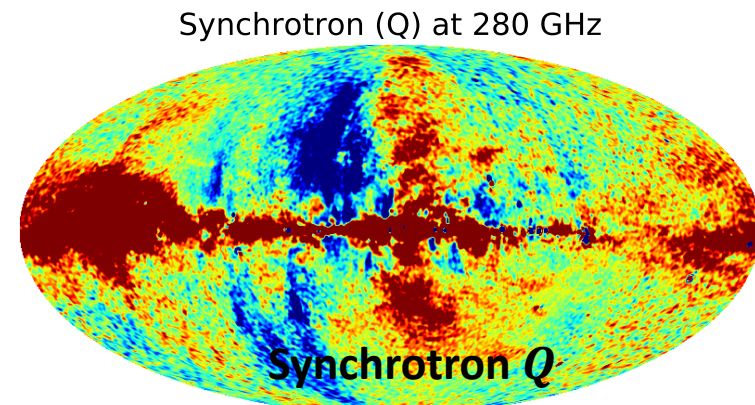
Foregrounds simulation (polarization)



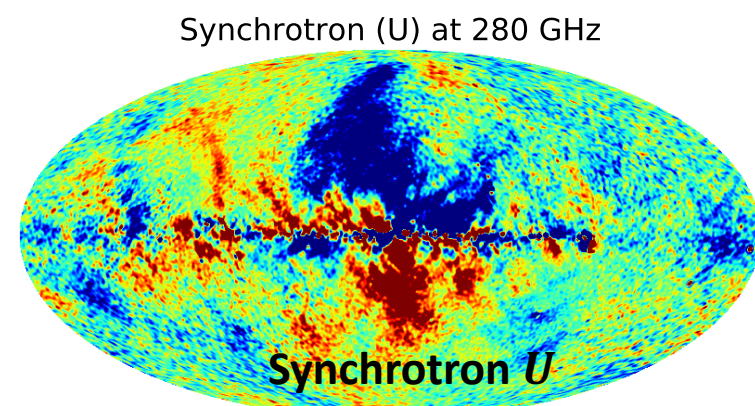
-100 μK_{CMB} 100



-100 μK_{CMB} 100



-0.1 μK_{CMB} 0.1

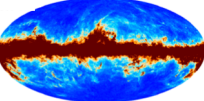


-0.1 μK_{CMB} 0.1

*Remazeilles, Ravenni, Chluba
(2110.14664)*

Component separation: classic ILC ?

$$d(\nu, \vec{n}) = \mathbf{a}(\nu) \mu(\vec{n}) + \mathbf{b}(\nu) T(\vec{n}) + \text{foregrounds}(\nu, \vec{n}) + \text{noise}(\nu, \vec{n})$$

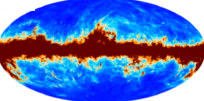
data ↓ ↓
 *μ -distortion
anisotropies* *CMB temperature
anisotropies*

The classic ILC method forms an estimate of the μ -map as

$$\hat{\mu}(\vec{n}) = \sum_{\nu} w(\nu) d(\nu, \vec{n}) \quad \text{such that} \quad \left\{ \begin{array}{l} \langle \hat{\mu}(\vec{n})^2 \rangle \text{ of minimum variance} \\ \sum_{\nu} w(\nu) \mathbf{a}(\nu) = \mathbf{1} \end{array} \right.$$

Component separation: classic ILC ?

$$d(\nu, \vec{n}) = \mathbf{a}(\nu) \mu(\vec{n}) + \mathbf{b}(\nu) T(\vec{n}) + \text{foregrounds}(\nu, \vec{n}) + \text{noise}(\nu, \vec{n})$$

data ↓ ↓
 *μ -distortion
anisotropies* *CMB temperature
anisotropies*

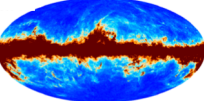
The classic ILC method forms an estimate of the μ -map as

$$\hat{\mu}(\vec{n}) = \sum_{\nu} w(\nu) d(\nu, \vec{n}) \quad \text{such that} \quad \left\{ \begin{array}{l} \langle \hat{\mu}(\vec{n})^2 \rangle \text{ of minimum variance} \\ \sum_{\nu} w(\nu) \mathbf{a}(\nu) = \mathbf{1} \end{array} \right.$$

$$\hat{\mu}(\vec{n}) = \left(\sum_{\nu} w(\nu) \mathbf{a}(\nu) \right) \mu(\vec{n}) + \left(\sum_{\nu} w(\nu) \mathbf{b}(\nu) \right) T(\vec{n}) + \dots$$

Component separation: classic ILC ?

$$d(\nu, \vec{n}) = \mathbf{a}(\nu) \mu(\vec{n}) + \mathbf{b}(\nu) T(\vec{n}) + \text{foregrounds}(\nu, \vec{n}) + \text{noise}(\nu, \vec{n})$$

data ↓ ↓
 *μ -distortion
anisotropies* *CMB temperature
anisotropies*

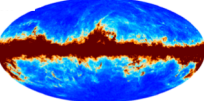
The classic ILC method forms an estimate of the μ -map as

$$\hat{\mu}(\vec{n}) = \sum_{\nu} w(\nu) d(\nu, \vec{n}) \quad \text{such that} \quad \left\{ \begin{array}{l} \langle \hat{\mu}(\vec{n})^2 \rangle \text{ of minimum variance} \\ \sum_{\nu} w(\nu) \mathbf{a}(\nu) = \mathbf{1} \end{array} \right.$$

$$\hat{\mu}(\vec{n}) = \underbrace{\left(\sum_{\nu} w(\nu) \mathbf{a}(\nu) \right)}_{= \mathbf{1}} \mu(\vec{n}) + \left(\sum_{\nu} w(\nu) \mathbf{b}(\nu) \right) T(\vec{n}) + \dots$$

Component separation: classic ILC ?

$$d(\nu, \vec{n}) = \mathbf{a}(\nu) \mu(\vec{n}) + \mathbf{b}(\nu) T(\vec{n}) + \text{foregrounds}(\nu, \vec{n}) + \text{noise}(\nu, \vec{n})$$

data ↓ ↓
 *μ -distortion
anisotropies* *CMB temperature
anisotropies*

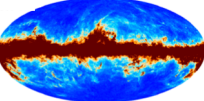
The classic ILC method forms an estimate of the μ -map as

$$\hat{\mu}(\vec{n}) = \sum_{\nu} w(\nu) d(\nu, \vec{n}) \quad \text{such that} \quad \left\{ \begin{array}{l} \langle \hat{\mu}(\vec{n})^2 \rangle \text{ of minimum variance} \\ \sum_{\nu} w(\nu) \mathbf{a}(\nu) = \mathbf{1} \end{array} \right.$$

$$\hat{\mu}(\vec{n}) = \mu(\vec{n}) + \left(\sum_{\nu} w(\nu) \mathbf{b}(\nu) \right) T(\vec{n}) + \dots$$

Component separation: classic ILC ?

$$d(\nu, \vec{n}) = \mathbf{a}(\nu) \mu(\vec{n}) + \mathbf{b}(\nu) T(\vec{n}) + \text{foregrounds}(\nu, \vec{n}) + \text{noise}(\nu, \vec{n})$$

data ↓ ↓
 *μ -distortion
anisotropies* *CMB temperature
anisotropies*

The classic ILC method forms an estimate of the μ -map as

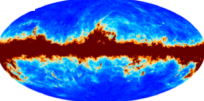
$$\hat{\mu}(\vec{n}) = \sum_{\nu} w(\nu) d(\nu, \vec{n}) \quad \text{such that} \quad \left\{ \begin{array}{l} \langle \hat{\mu}(\vec{n})^2 \rangle \text{ of minimum variance} \\ \sum_{\nu} w(\nu) \mathbf{a}(\nu) = \mathbf{1} \end{array} \right.$$

residual CMB anisotropies!

$$\hat{\mu}(\vec{n}) = \mu(\vec{n}) + \overbrace{\left(\sum_{\nu} w(\nu) \mathbf{b}(\nu) \right) T(\vec{n})}^{\text{residual CMB anisotropies!}} + \dots$$

Component separation: classic ILC ?

$$d(\nu, \vec{n}) = \mathbf{a}(\nu) \mu(\vec{n}) + \mathbf{b}(\nu) T(\vec{n}) + \text{foregrounds}(\nu, \vec{n}) + \text{noise}(\nu, \vec{n})$$

data ↓ ↓
 *μ -distortion
anisotropies* *CMB temperature
anisotropies*

The classic ILC method forms an estimate of the μ -map as

$$\hat{\mu}(\vec{n}) = \sum_{\nu} w(\nu) d(\nu, \vec{n}) \quad \text{such that} \quad \left\{ \begin{array}{l} \langle \hat{\mu}(\vec{n})^2 \rangle \text{ of minimum variance} \\ \sum_{\nu} w(\nu) \mathbf{a}(\nu) = \mathbf{1} \end{array} \right.$$

residual CMB anisotropies!

$$\hat{\mu}(\vec{n}) = \mu(\vec{n}) + \overbrace{\left(\sum_{\nu} w(\nu) \mathbf{b}(\nu) \right) T(\vec{n})}^{\text{residual CMB anisotropies!}} + \dots$$

$$\Rightarrow C_{\ell}^{\hat{\mu} \times \hat{T}} = C_{\ell}^{\mu T} + \varepsilon C_{\ell}^{TT} + \dots$$

Component separation: classic ILC ?

$$d(\nu, \vec{n}) = \mathbf{a}(\nu) \mu(\vec{n}) + \mathbf{b}(\nu) T(\vec{n}) + \text{foregrounds}(\nu, \vec{n}) + \text{noise}(\nu, \vec{n})$$

↓ ↓
data *μ -distortion
anisotropies* *CMB temperature
anisotropies*

The classic ILC method forms an estimate of the μ -map as

$$\hat{\mu}(\vec{n}) = \sum_{\nu} w(\nu) d(\nu, \vec{n}) \quad \text{such that} \quad \begin{cases} \langle \hat{\mu}(\vec{n})^2 \rangle \text{ of minimum variance} \\ \sum_{\nu} w(\nu) \mathbf{a}(\nu) = \mathbf{1} \end{cases}$$

residual CMB anisotropies!

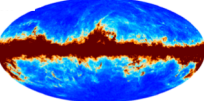
$$\hat{\mu}(\vec{n}) = \mu(\vec{n}) + \overbrace{\left(\sum_{\nu} w(\nu) \mathbf{b}(\nu) \right) T(\vec{n})}^{\text{residual CMB anisotropies!}} + \dots$$

$$\Rightarrow C_{\ell}^{\hat{\mu} \times \hat{T}} = C_{\ell}^{\mu T} + \varepsilon C_{\ell}^{TT} + \dots$$

*residual
TT correlations!*

Component separation: constrained ILC !

$$d(\nu, \vec{n}) = \mathbf{a}(\nu) \mu(\vec{n}) + \mathbf{b}(\nu) T(\vec{n}) + \text{foregrounds}(\nu, \vec{n}) + \text{noise}(\nu, \vec{n})$$

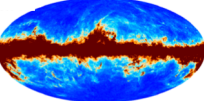
data ↓ ↓

*μ-distortion
anisotropies* *CMB temperature
anisotropies*

The classic ILC **constrained ILC** method forms an estimate of the μ -map as

$$\hat{\mu}(\vec{n}) = \sum_{\nu} w(\nu) d(\nu, \vec{n}) \quad \text{such that} \quad \left\{ \begin{array}{l} \langle \hat{\mu}(\vec{n})^2 \rangle \text{ of minimum variance} \\ \sum_{\nu} w(\nu) \mathbf{a}(\nu) = \mathbf{1} \\ \sum_{\nu} w(\nu) \mathbf{b}(\nu) = \mathbf{0} \end{array} \right.$$

Component separation: constrained ILC !

$$d(\nu, \vec{n}) = \mathbf{a}(\nu) \mu(\vec{n}) + \mathbf{b}(\nu) T(\vec{n}) + \text{foregrounds}(\nu, \vec{n}) + \text{noise}(\nu, \vec{n})$$

data ↓ ↓

 *μ -distortion
anisotropies* *CMB temperature
anisotropies*

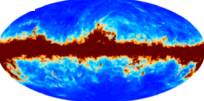
The classic ILC **constrained ILC** method forms an estimate of the μ -map as

$$\hat{\mu}(\vec{n}) = \sum_{\nu} w(\nu) d(\nu, \vec{n}) \quad \text{such that} \quad \left\{ \begin{array}{l} \langle \hat{\mu}(\vec{n})^2 \rangle \text{ of minimum variance} \\ \sum_{\nu} w(\nu) \mathbf{a}(\nu) = \mathbf{1} \\ \boxed{\sum_{\nu} w(\nu) \mathbf{b}(\nu) = \mathbf{0}} \end{array} \right.$$

Extra constraint to guarantee the cancellation of CMB residuals

Component separation: constrained ILC !

$$d(\nu, \vec{n}) = \mathbf{a}(\nu) \mu(\vec{n}) + \mathbf{b}(\nu) T(\vec{n}) + \text{foregrounds}(\nu, \vec{n}) + \text{noise}(\nu, \vec{n})$$

↓
 data μ -distortion

 anisotropies CMB temperature
 anisotropies

The classic ILC **constrained ILC** method forms an estimate of the μ -map as

$$\hat{\mu}(\vec{n}) = \sum_{\nu} w(\nu) d(\nu, \vec{n}) \quad \text{such that} \quad \begin{cases} \langle \hat{\mu}(\vec{n})^2 \rangle \text{ of minimum variance} \\ \sum_{\nu} w(\nu) \mathbf{a}(\nu) = \mathbf{1} \\ \sum_{\nu} w(\nu) \mathbf{b}(\nu) = \mathbf{0} \end{cases}$$

$$\begin{aligned} \hat{\mu}(\vec{n}) &= \mu(\vec{n}) + \underbrace{\left(\sum_{\nu} w(\nu) \mathbf{b}(\nu) \right)}_{=0} T(\vec{n}) + \dots \\ \Rightarrow C_{\ell}^{\hat{\mu} \times T} &= C_{\ell}^{\mu \times T} + \cancel{\mathcal{E}_{\ell}^{TT}} + \dots \end{aligned}$$

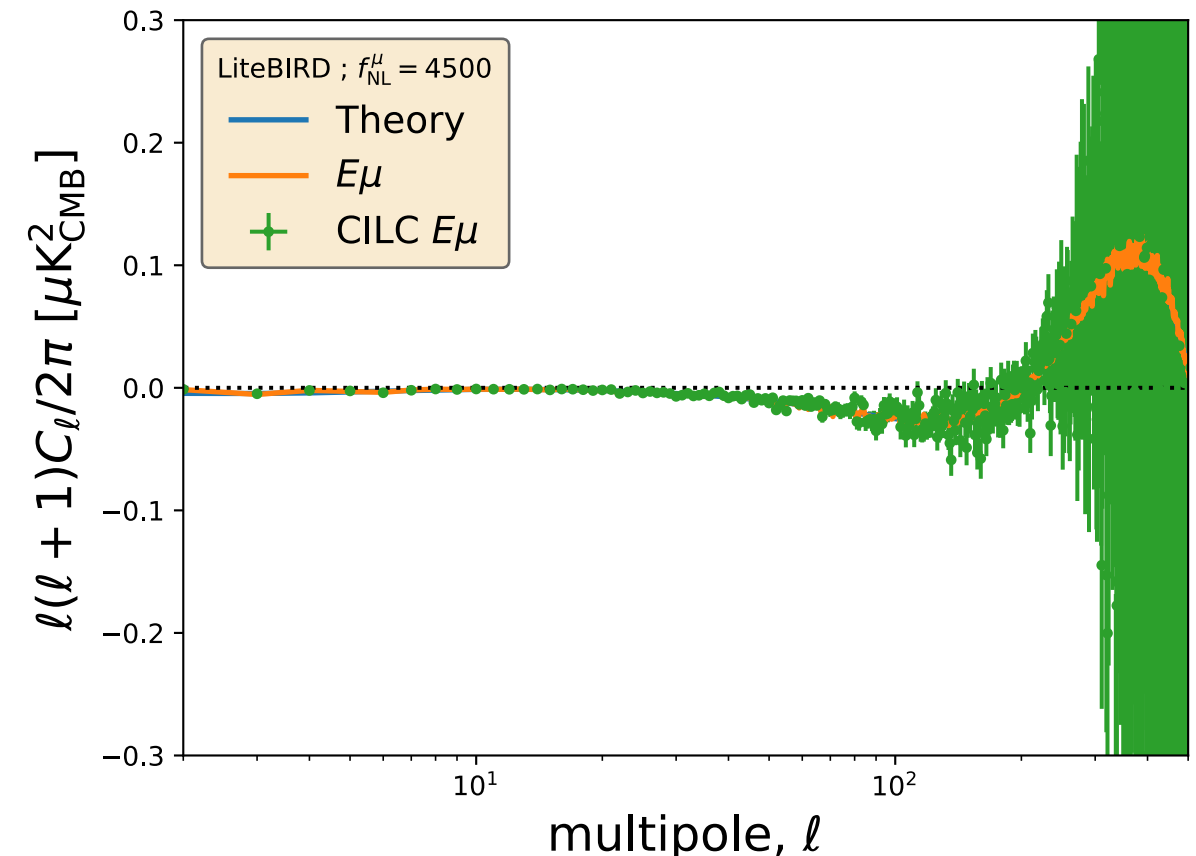
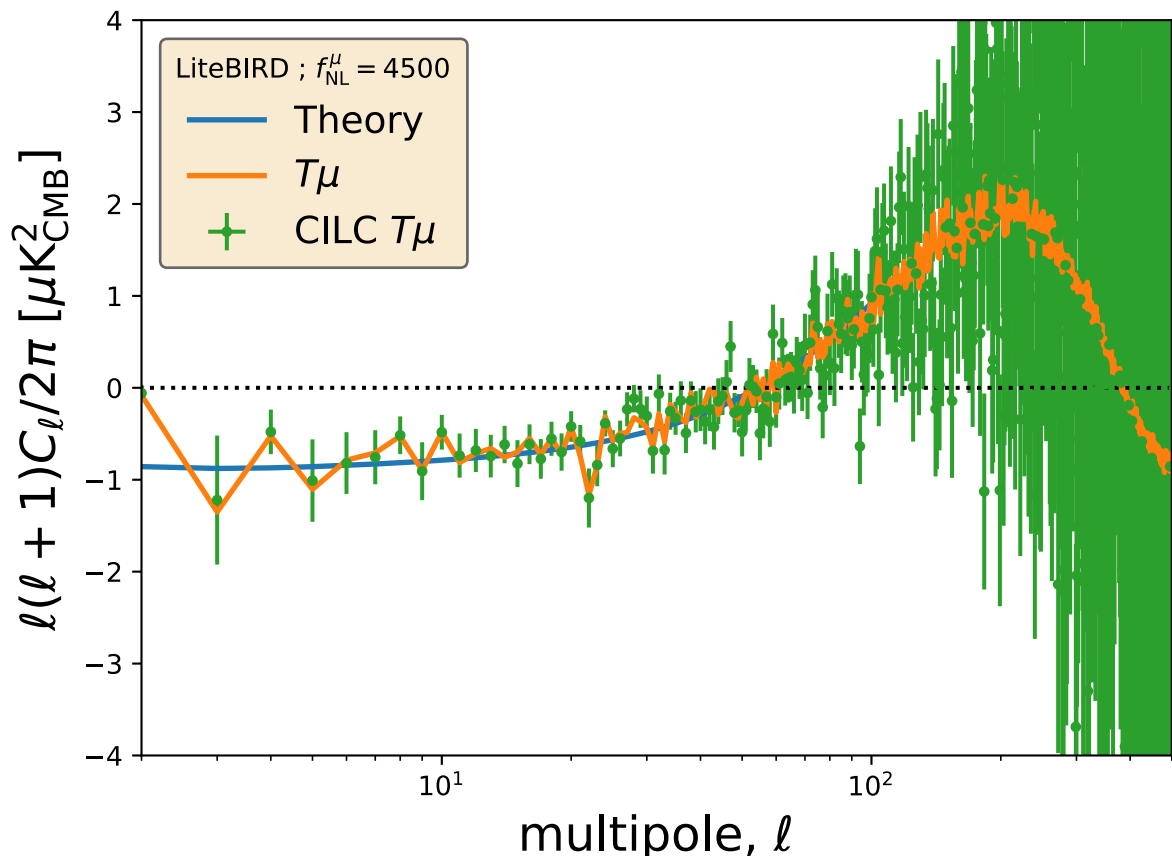
*Zero residual
TT correlation!*

Results

No binning

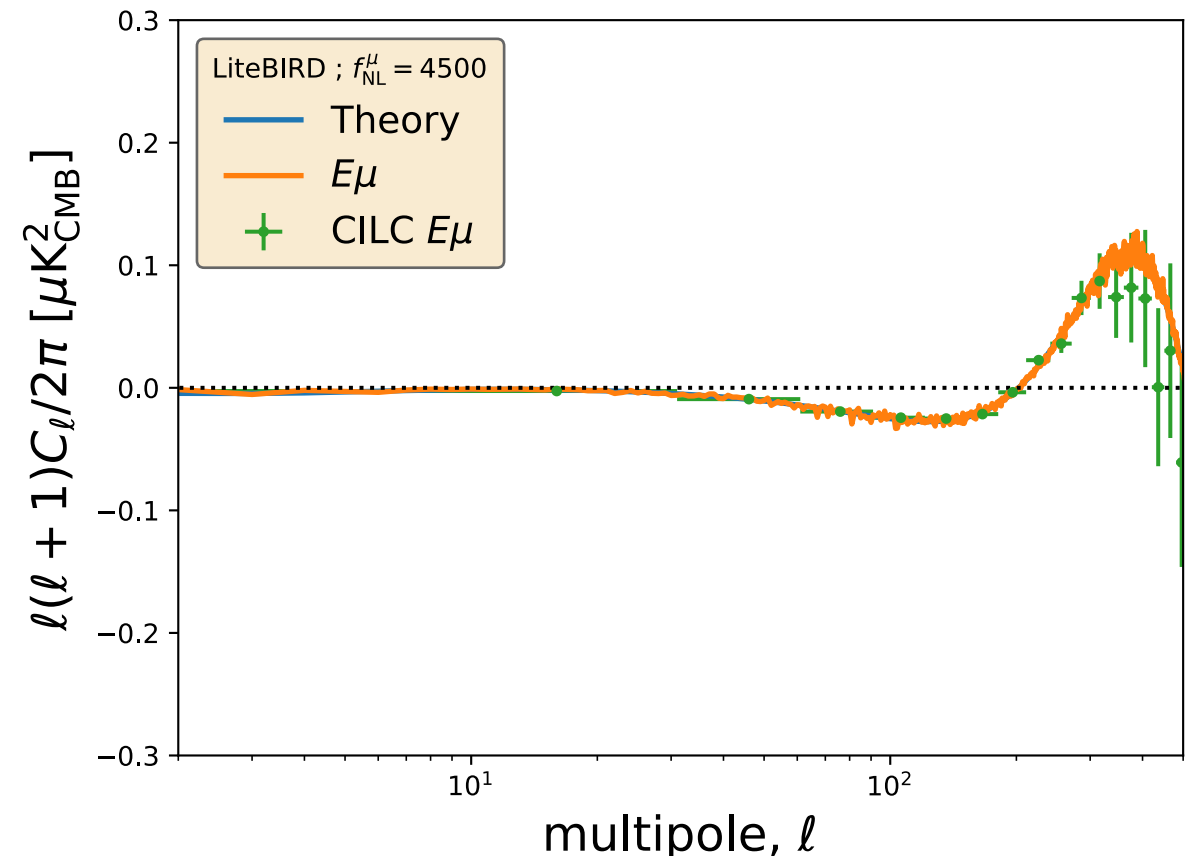
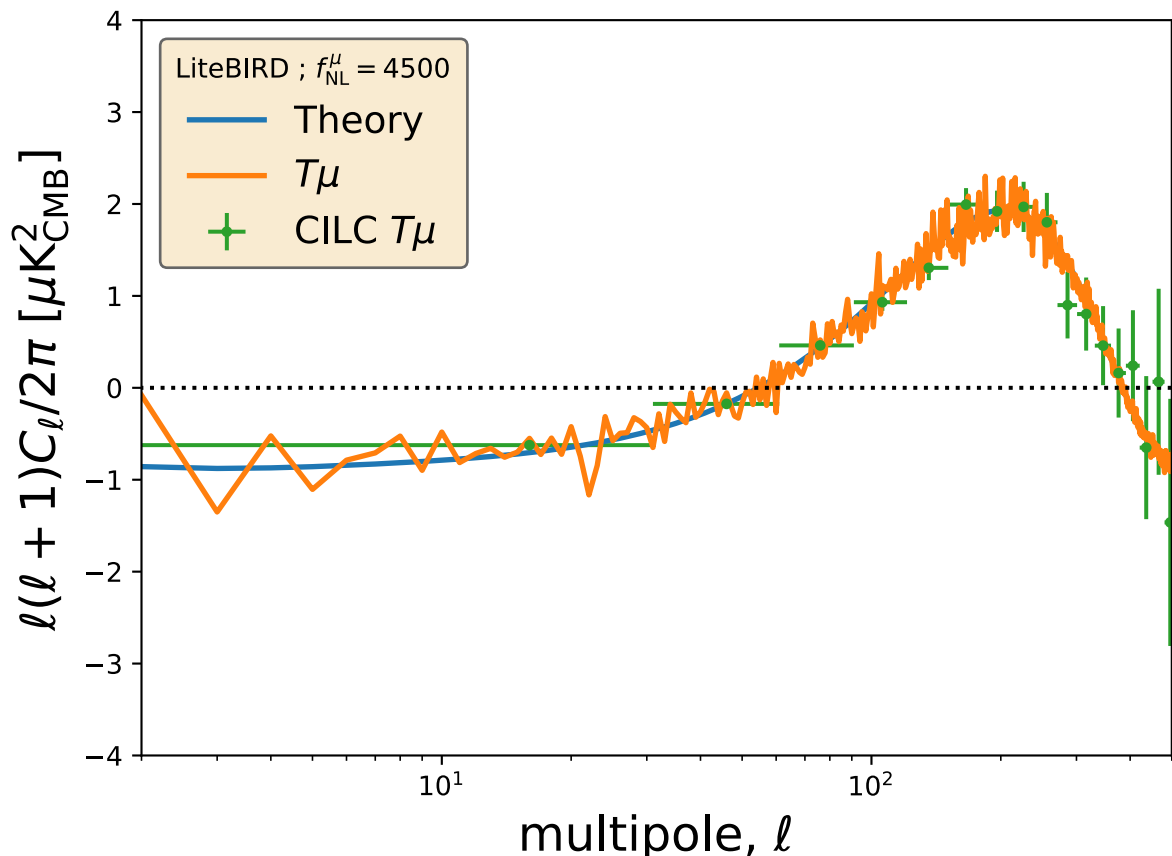
LiteBIRD, $f_{NL}^\mu = 4500$ without foregrounds

Remazeilles,
Ravenni, Chluba
(2110.14664)

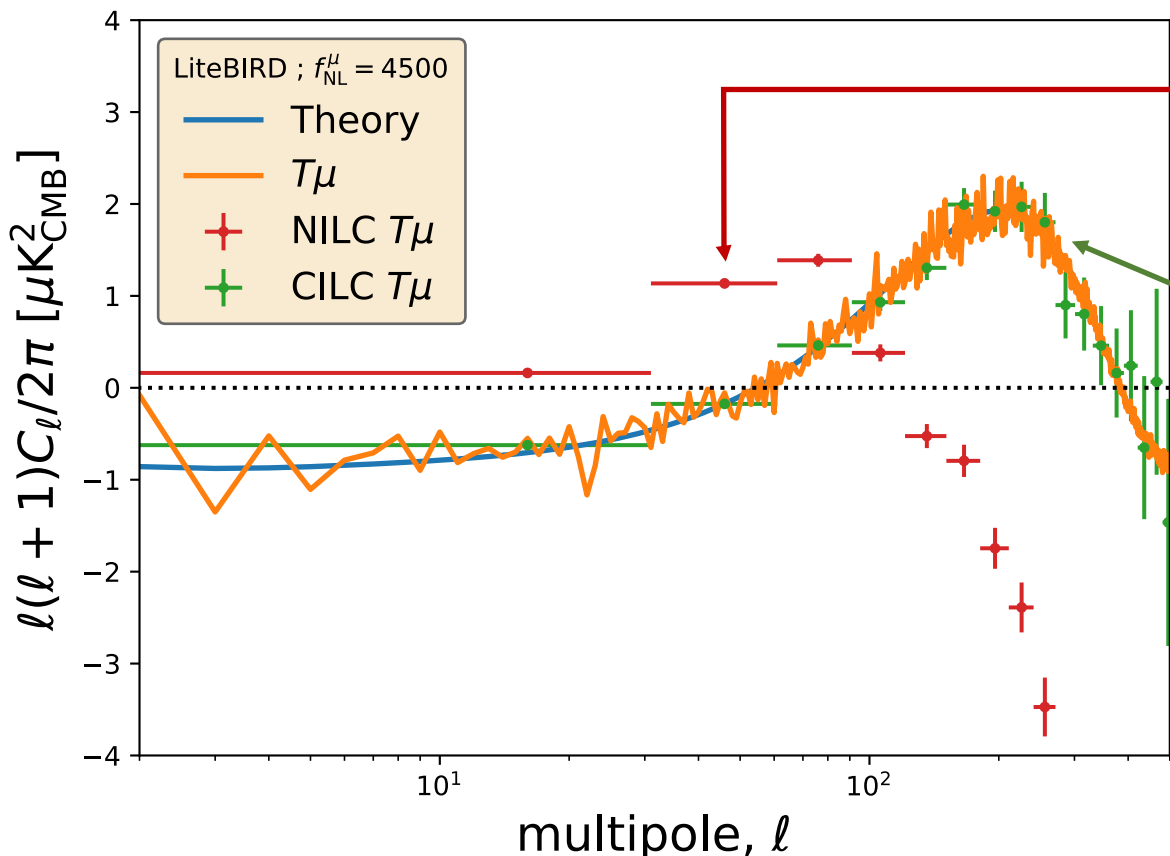


LiteBIRD, $f_{NL}^{\mu} = 4500$ without foregrounds

Remazeilles,
Ravenni, Chluba
(2110.14664)



Classic ILC vs Constrained ILC



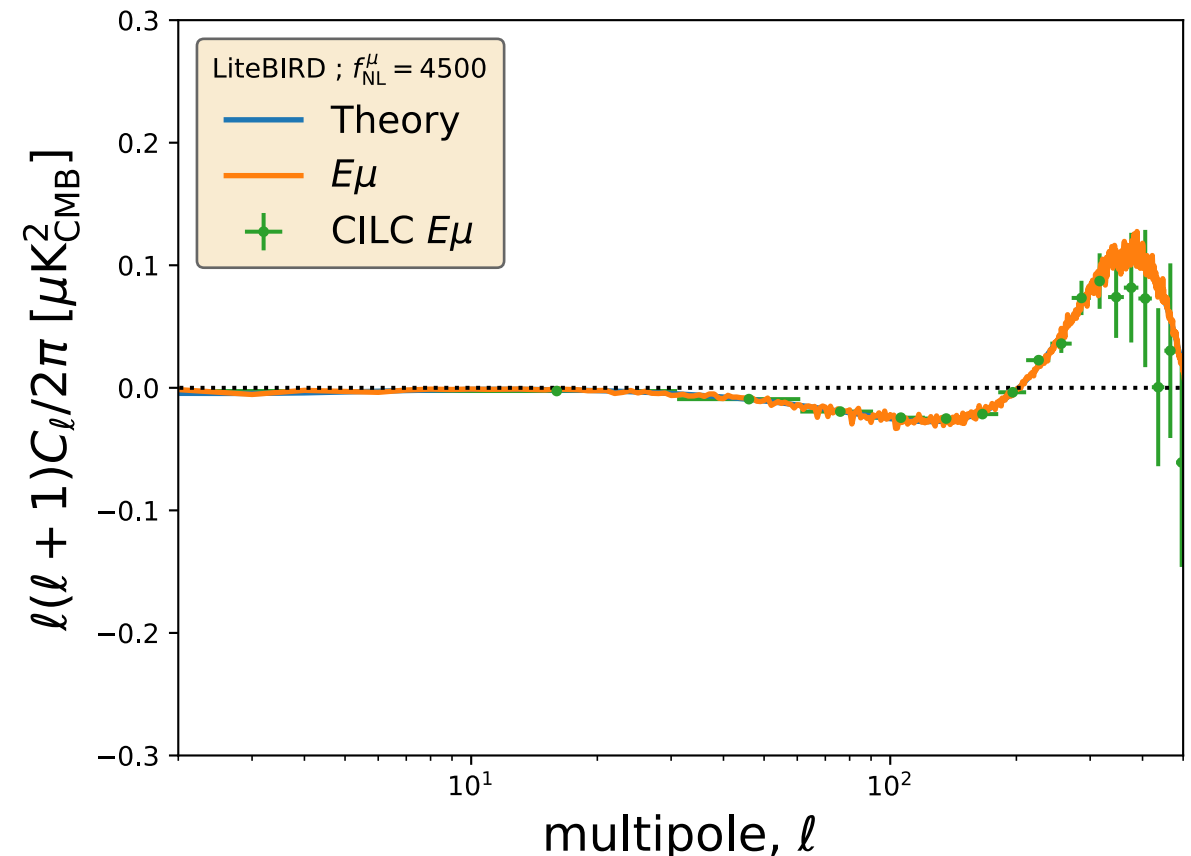
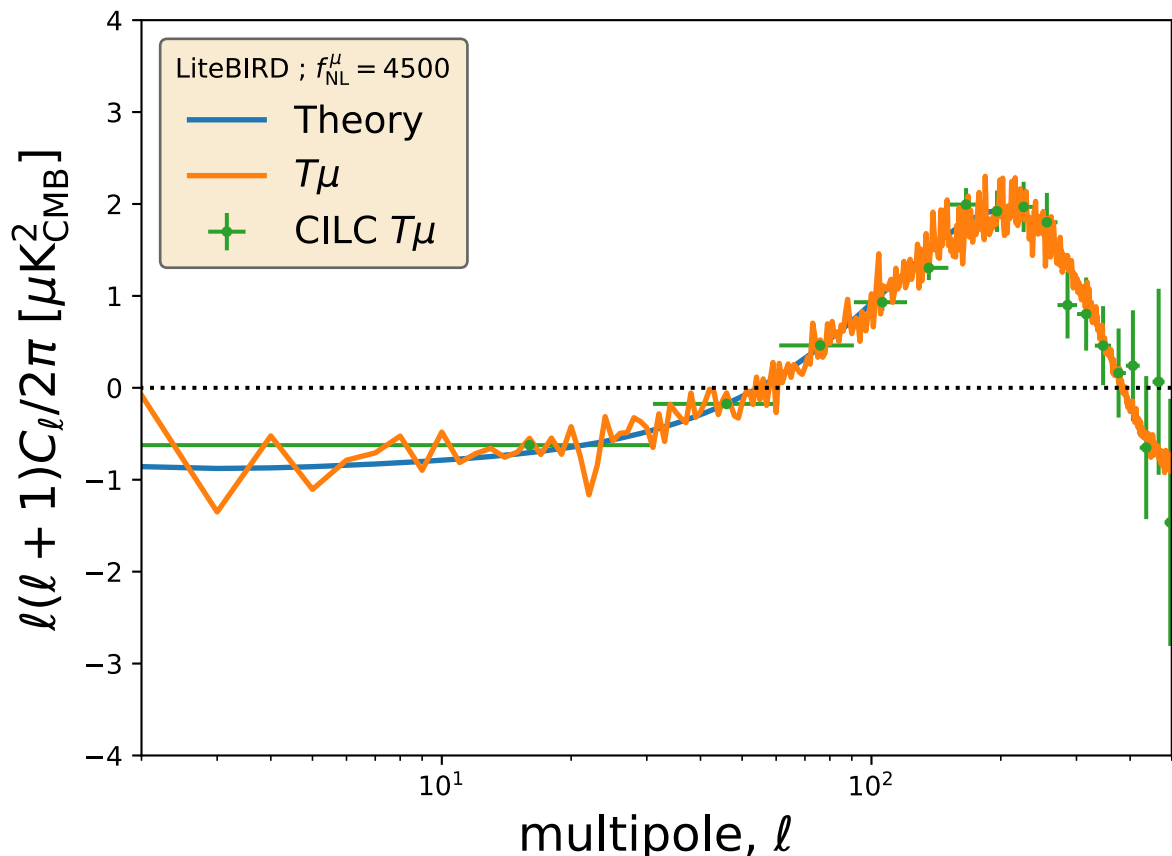
Classic ILC methods suffer from spurious TT correlations due to residual CMB anisotropies in the μ -map

The Constrained ILC fully recovers the correlated μT signal without bias

Remazeilles, Ravenni, Chluba (2110.14664)
Remazeilles & Chluba, MNRAS 2018

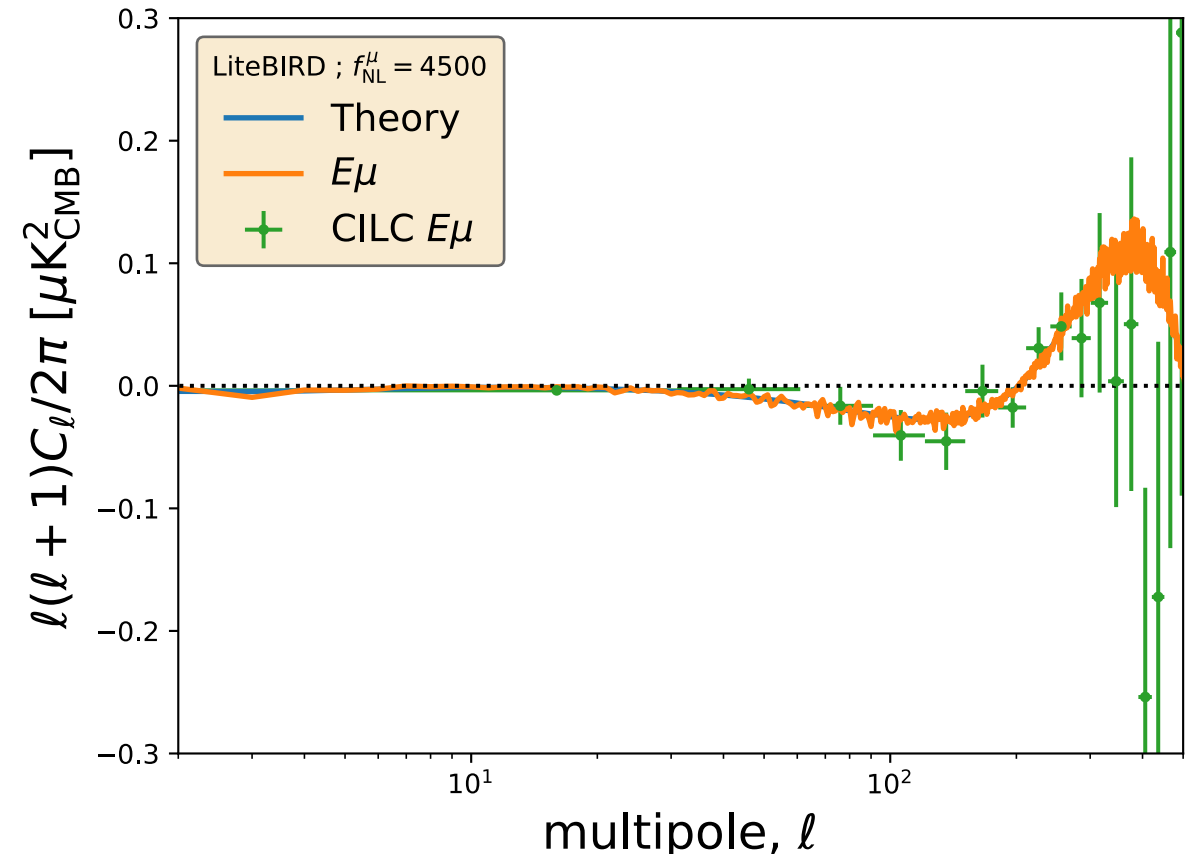
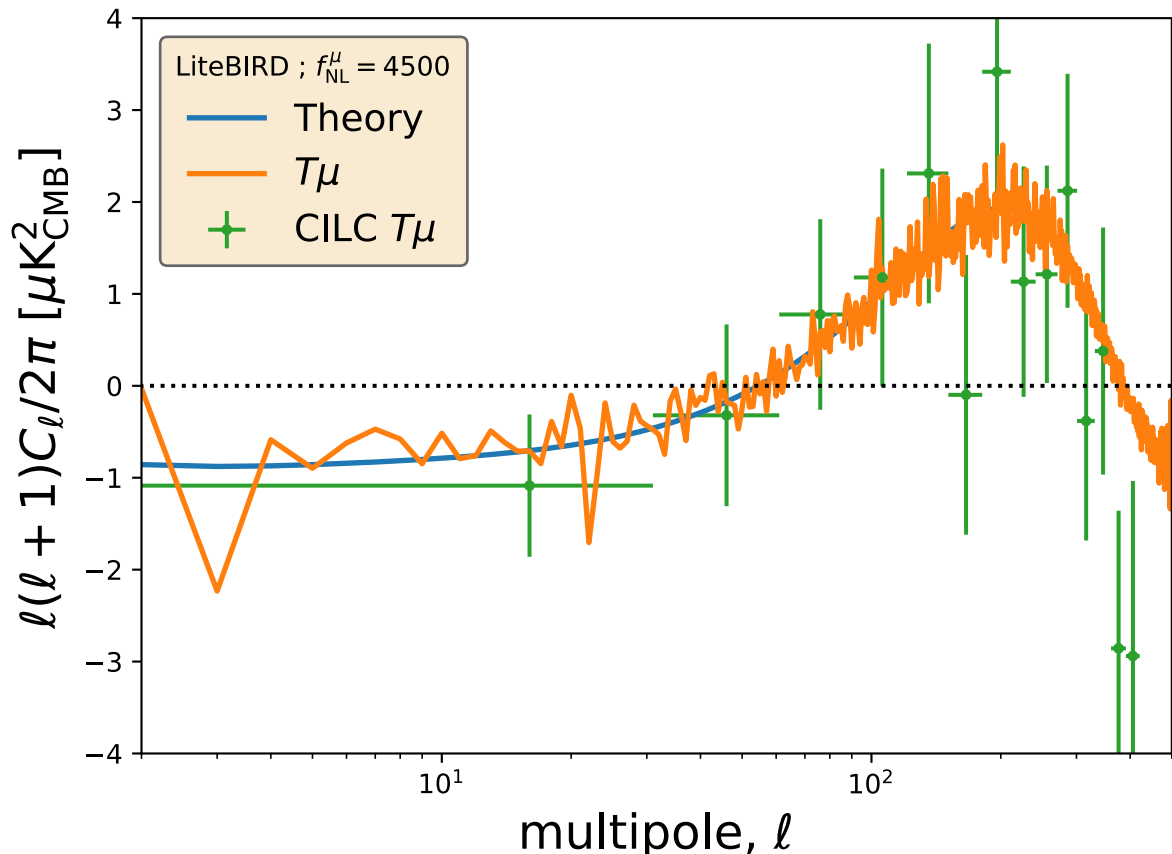
LiteBIRD, $f_{NL}^{\mu} = 4500$ without foregrounds

Remazeilles,
Ravenni, Chluba
(2110.14664)



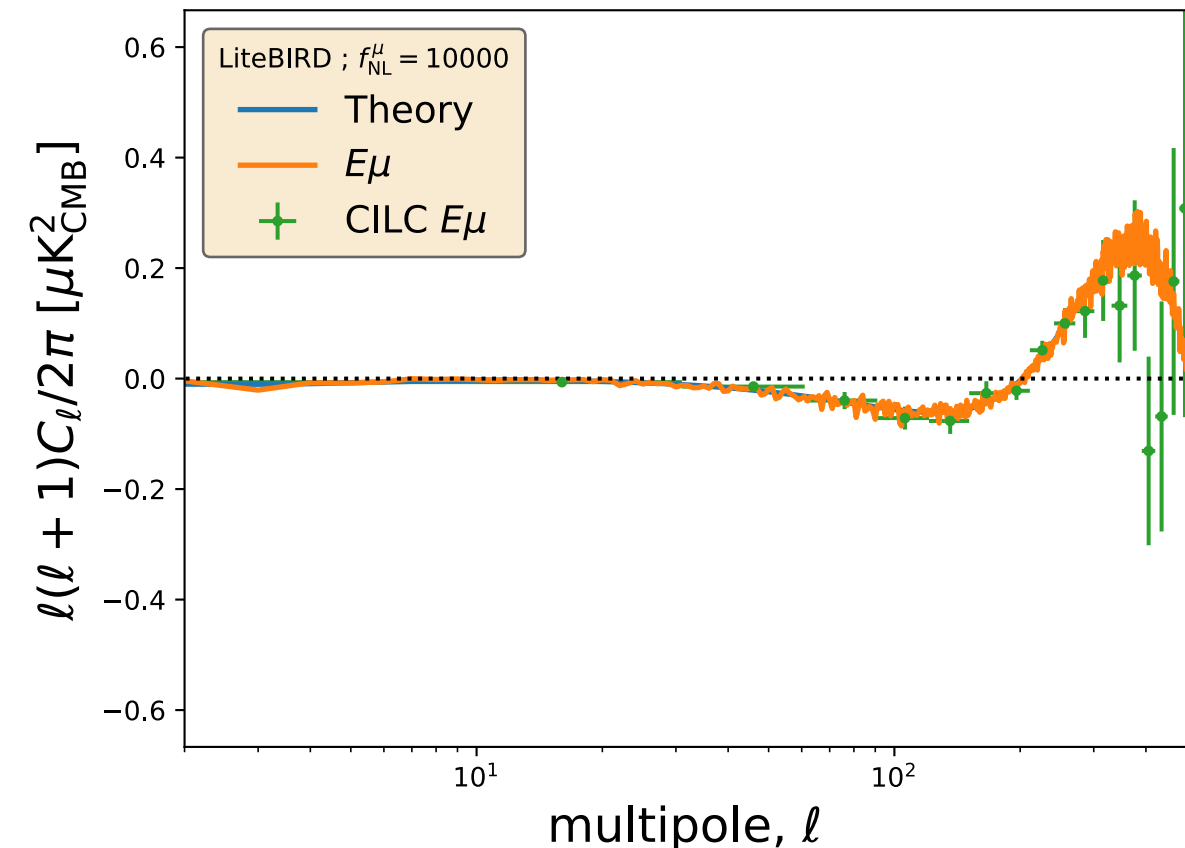
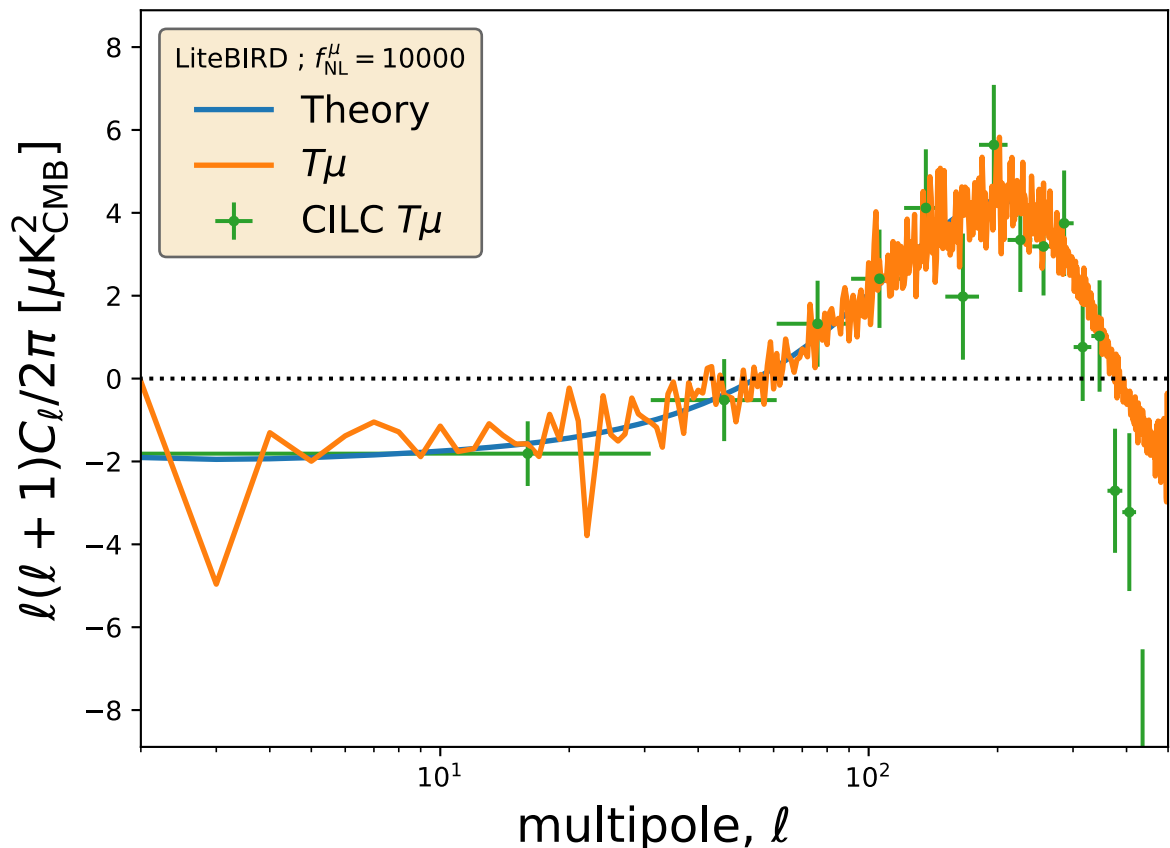
LiteBIRD, $f_{NL}^{\mu} = 4500$ with foregrounds

Remazeilles,
Ravenni, Chluba
(2110.14664)



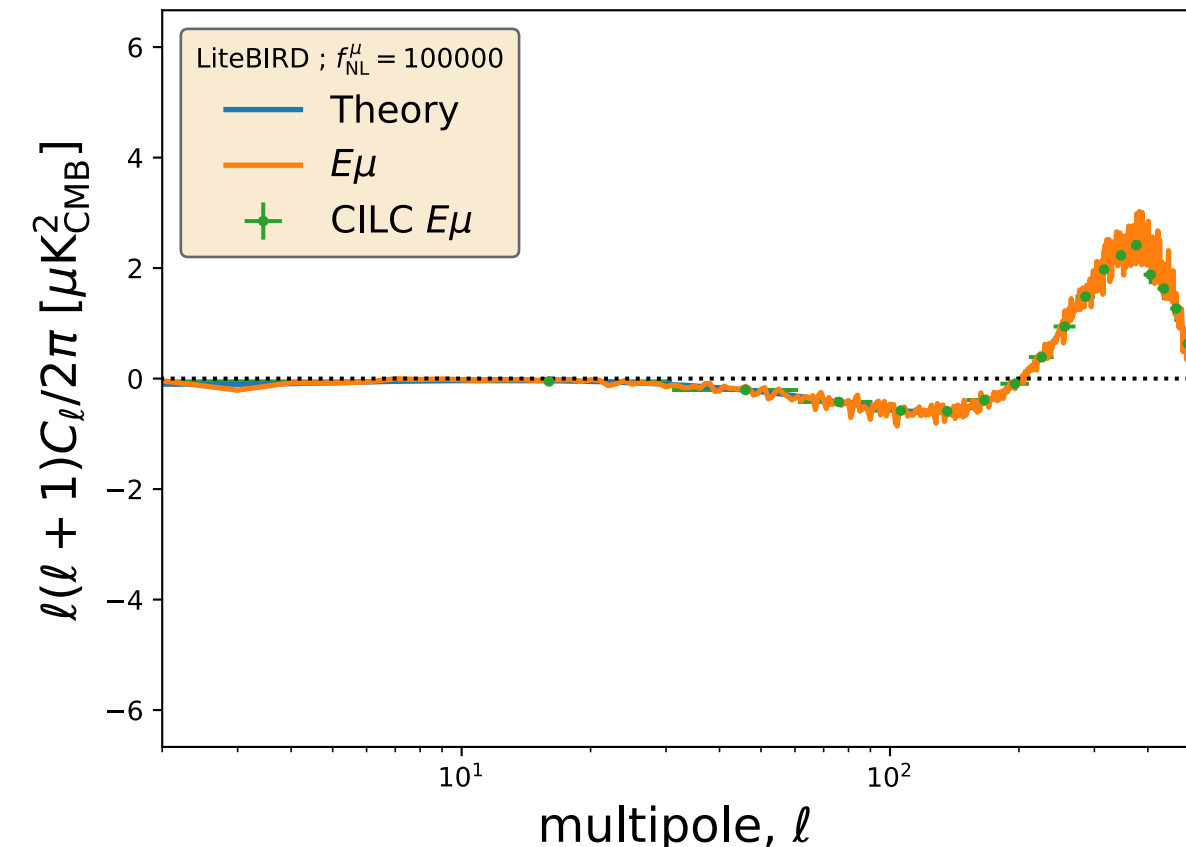
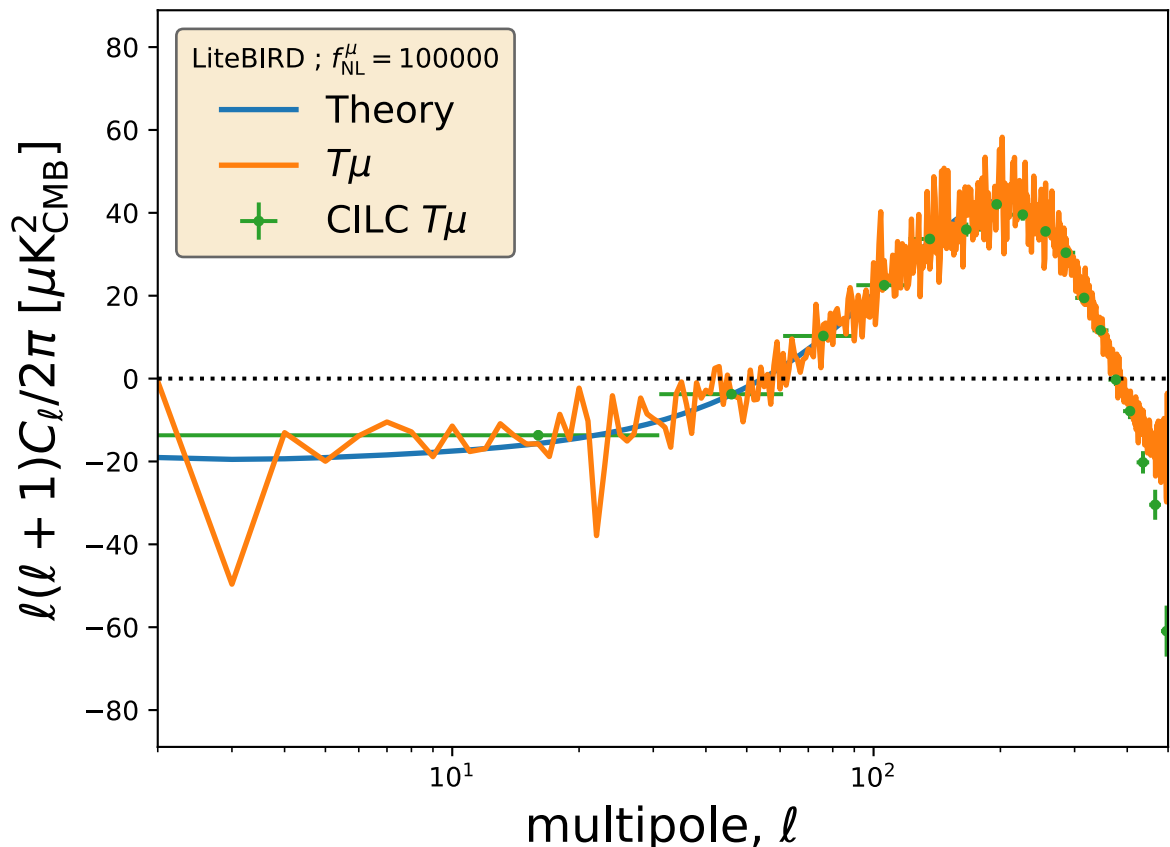
LiteBIRD, $f_{NL}^\mu = 10^4$ with foregrounds

Remazeilles,
Ravenni, Chluba
(2110.14664)



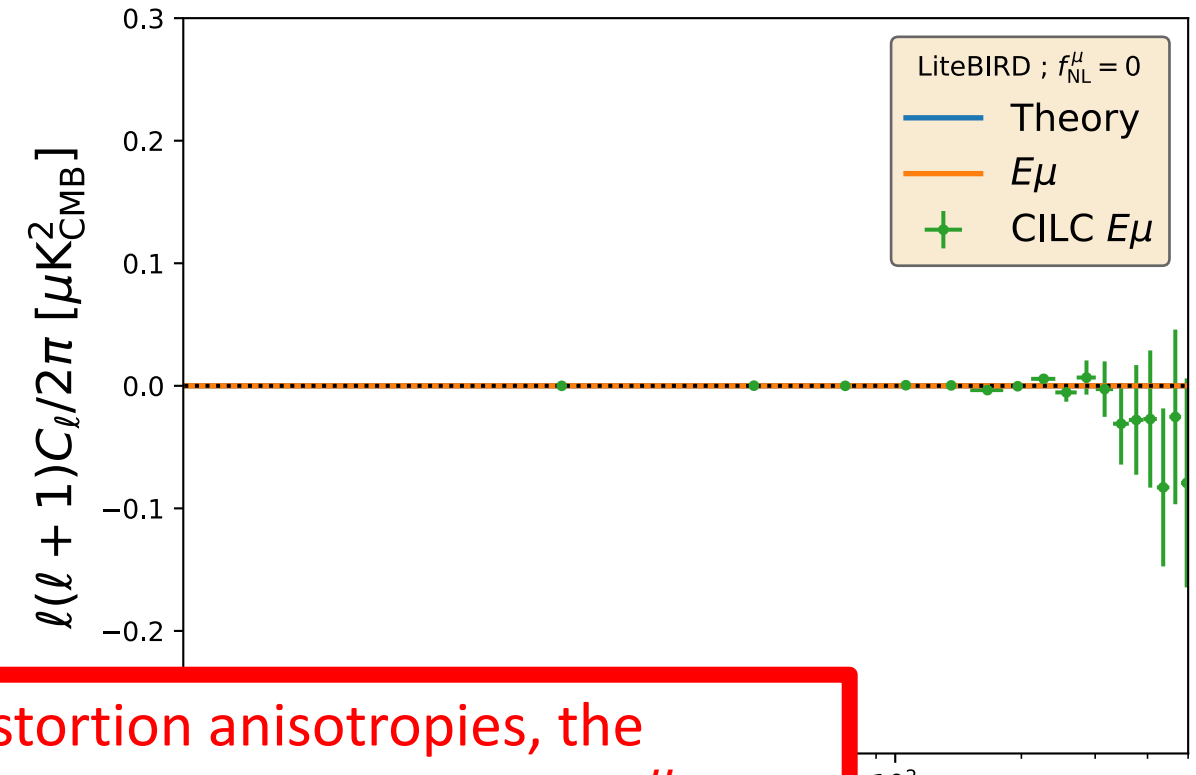
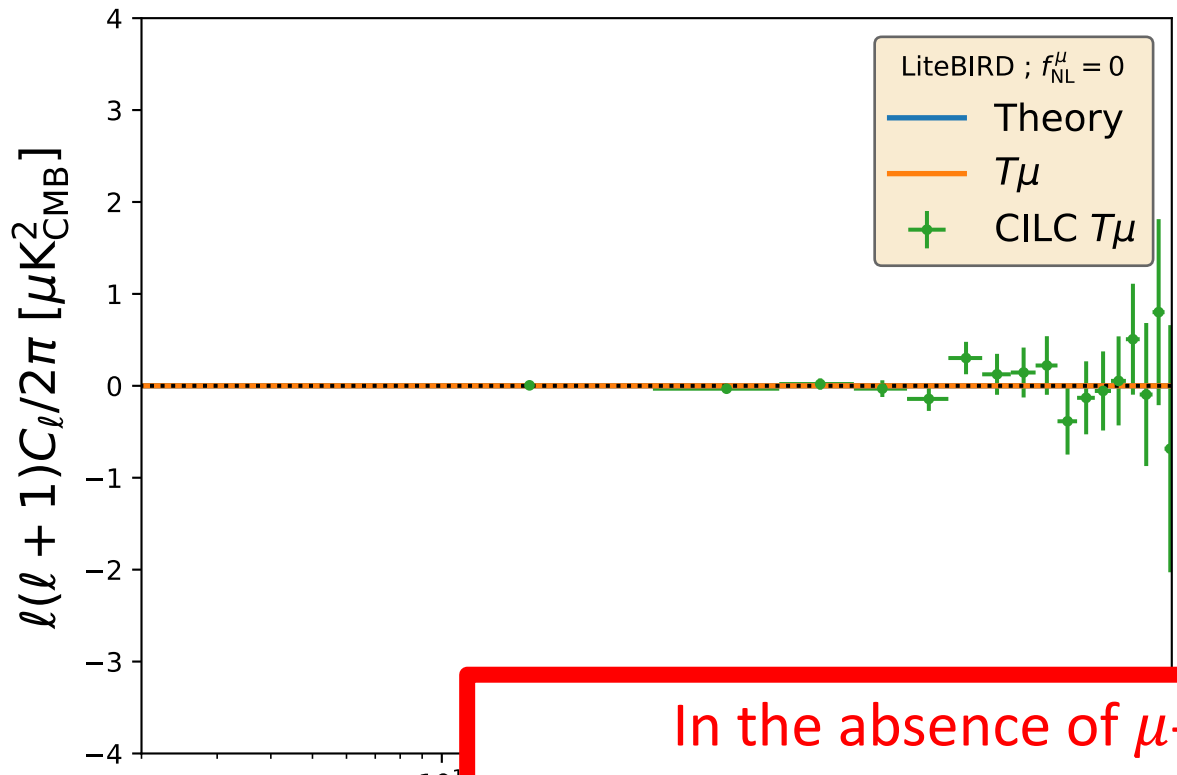
LiteBIRD, $f_{NL}^\mu = 10^5$ with foregrounds

Remazeilles,
Ravenni, Chluba
(2110.14664)



LiteBIRD null test, $f_{NL}^\mu = 0$ without foregrounds

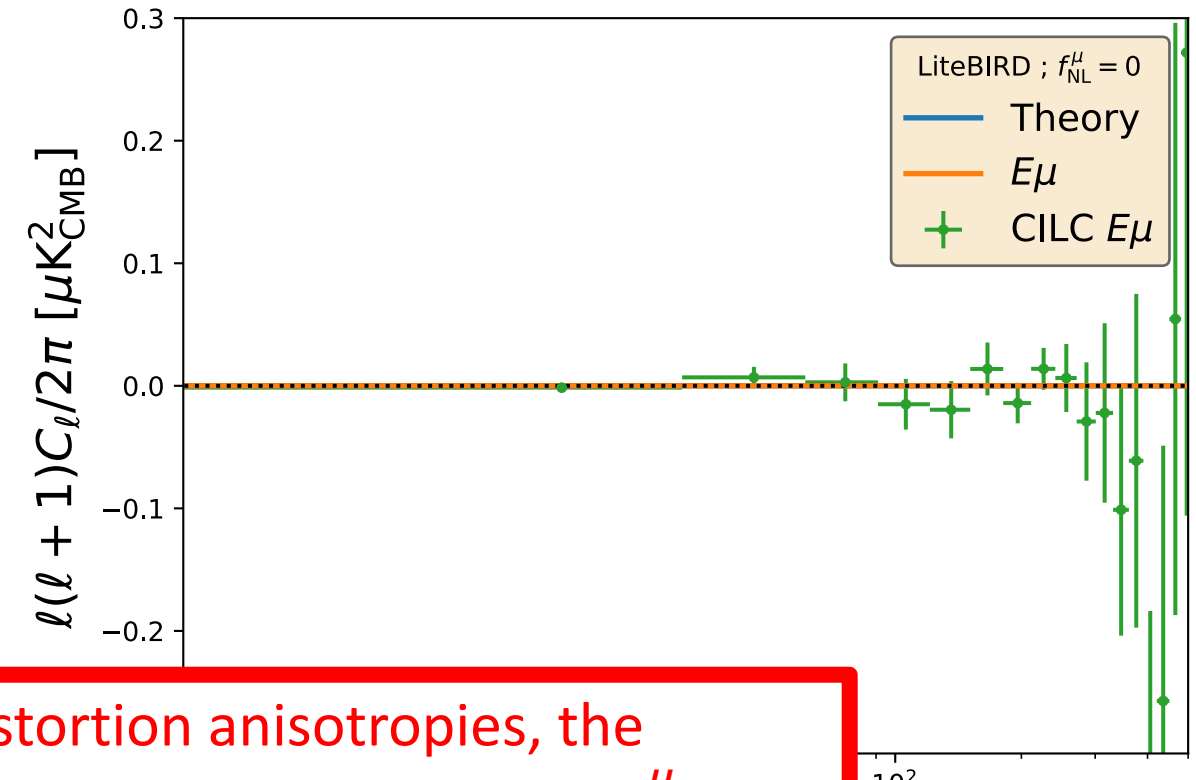
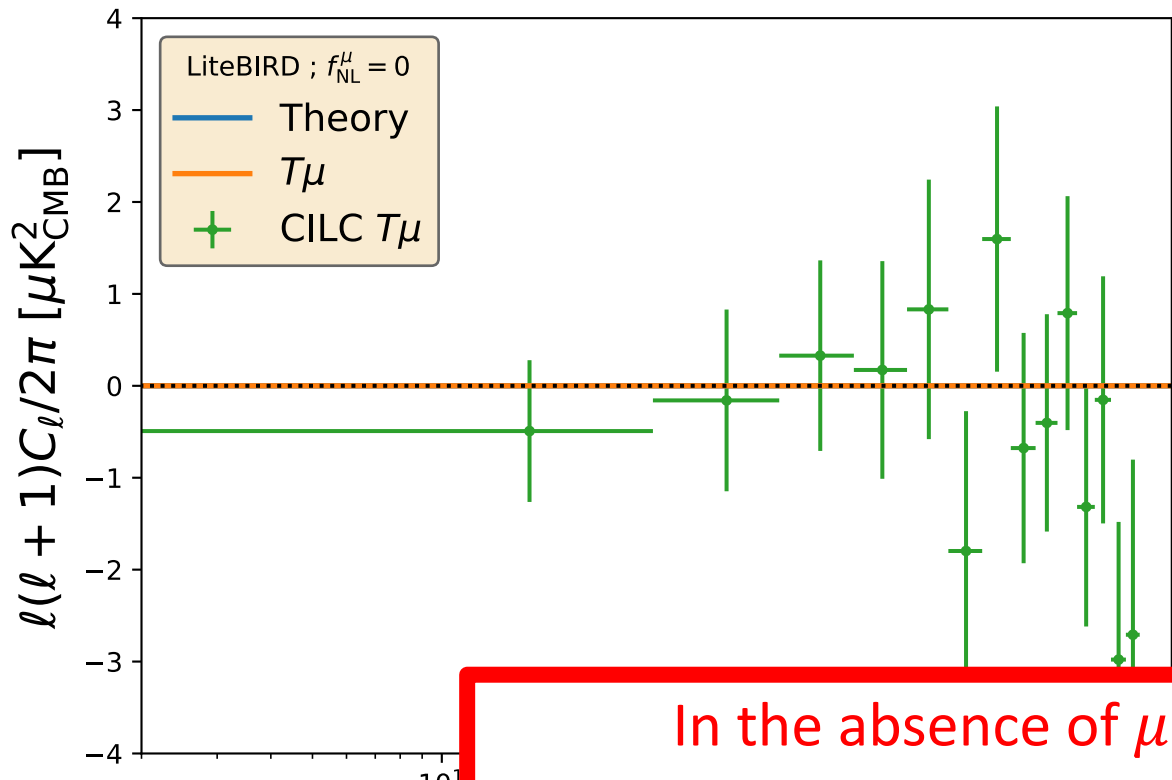
Remazeilles,
Ravenni, Chluba
(2110.14664)



In the absence of μ -distortion anisotropies, the reconstruction by Constrained ILC is consistent with $f_{NL}^\mu = 0$

LiteBIRD null test, $f_{NL}^\mu = 0$ with foregrounds

Remazeilles,
Ravenni, Chluba
(2110.14664)



In the absence of μ -distortion anisotropies, the reconstruction by Constrained ILC is consistent with $f_{NL}^\mu = 0$

Forecasts on $f_{NL}^\mu(k \simeq 740 \text{ Mpc}^{-1})$

$\mu \times T$

Remazeilles, Ravenni, Chluba (2110.14664)

LiteBIRD simulation

f_{NL}^μ (fiducial)	10^5	10^4	4500	0	4500	0
$\mu \times T$	$(0.97 \pm 0.02) \times 10^5$	$(1.05 \pm 0.12) \times 10^4$	5264 ± 1286	951 ± 1286	4348 ± 152	8.2 ± 103
	[50 σ]	[8 σ]	[3.5 σ]	-	[30 σ]	-

Forecasts on $f_{NL}^\mu(k \simeq 740 \text{ Mpc}^{-1})$

$\mu \times T$

<i>Remazeilles, Ravenni, Chluba (2110.14664)</i>				<i>LiteBIRD simulation</i>		
f_{NL}^μ (fiducial)	10^5	10^4	4500	0	4500 (w/o foregrounds)	0 (w/o foregrounds)
$\mu \times T$	$(0.97 \pm 0.02) \times 10^5$ [50 σ]	$(1.05 \pm 0.12) \times 10^4$ [8 σ]	5264 \pm 1286 [3.5 σ]	951 \pm 1286 -	4348 \pm 152 [30 σ]	8.2 \pm 103 -

Foregrounds degrade the sensitivity to f_{NL}^μ by about a factor of 10

Forecasts on $f_{NL}^\mu(k \simeq 740 \text{ Mpc}^{-1})$

$\mu \times E$

<i>Remazeilles, Ravenni, Chluba (2110.14664)</i>					<i>LiteBIRD simulation</i>	
f_{NL}^μ (fiducial)	10^5	10^4	4500	0	4500 (w/o foregrounds)	0 (w/o foregrounds)
$\mu \times T$	$(0.97 \pm 0.02) \times 10^5$ [50 σ]	$(1.05 \pm 0.12) \times 10^4$ [8 σ]	5264 ± 1286 [3.5 σ]	951 ± 1286 -	4348 ± 152 [30 σ]	8.2 ± 103 -
$\mu \times E$	$(0.96 \pm 0.01) \times 10^5$ [100 σ]	$(0.91 \pm 0.11) \times 10^4$ [9 σ]	3779 ± 1089 [4 σ]	-534 ± 1084 -	4366 ± 108 [42 σ]	0.9 ± 76 -

μE provides more constraining power than μT on f_{NL}^μ

Forecasts on f_{NL}^μ ($k \simeq 740 \text{ Mpc}^{-1}$)

$\mu \times T, E$ (joint)

	<i>Remazeilles, Ravenni, Chluba (2110.14664)</i>				<i>LiteBIRD simulation</i>	
f_{NL}^μ (fiducial)	10^5	10^4	4500	0	4500 (w/o foregrounds)	0 (w/o foregrounds)
$\mu \times T$	$(0.97 \pm 0.02) \times 10^5$ [50 σ]	$(1.05 \pm 0.12) \times 10^4$ [8 σ]	5264 ± 1286 [3.5 σ]	951 ± 1286 -	4348 ± 152 [30 σ]	8.2 ± 103 -
$\mu \times E$	$(0.96 \pm 0.01) \times 10^5$ [100 σ]	$(0.91 \pm 0.11) \times 10^4$ [9 σ]	3779 ± 1089 [4 σ]	-534 ± 1084 -	4366 ± 108 [42 σ]	0.9 ± 76 -
$\mu \times T, E$ (joint)	$(0.97 \pm 0.01) \times 10^5$ [100 σ]	$(0.97 \pm 0.08) \times 10^4$ [11 σ]	4425 ± 827 [5 σ]	95 ± 824 -	4329 ± 90 [48 σ]	-2.8 ± 62 -

5σ detection of $f_{NL}^\mu = 4500$ after foreground cleaning

***LiteBIRD* detection limit $\sigma(f_{NL}^\mu = 0) \lesssim 800$ in the presence of foregrounds**

Takeaway

- ❑ The Constrained ILC method enables to recover μT and μE correlation signals without bias
- ❑ Foregrounds degrade the sensitivity to $f_{\text{NL}}^{\mu}(k \simeq 740 \text{ Mpc}^{-1})$ by a factor of 10
- ❑ *LiteBIRD* detection limit $\sigma(f_{\text{NL}}^{\mu} = 0) \lesssim 800$ from joint μT , μE analysis after foreground cleaning
- ❑ μE correlations provide more constraining power than μT correlations on f_{NL}^{μ} !
 - Because the degree of correlation between μ and E is larger than that of μ and T
 - Because foregrounds are less complex in polarization than in intensity
 - Because the CMB E -mode map is immune from μ -distortion anisotropies
- ❑ Using SD anisotropies, LiteBIRD may allow to shed light on scale-dependent non-Gaussianity and non-standard models of inflation:
 - Multi-field inflation *Dimastrogiovanni et al, JCAP 2016*
 - Non-Bunch-Davies initial conditions *Ganc & Komatsu, PRD 2012*